

1 **Secondary formation dominated low molecular weight amines origins**  
2 **in aerosols over the marginal seas of China**

3 Xiao-Ying Yang<sup>1,2</sup>, Fang Cao<sup>1,2</sup>, Chang-Liu Wu<sup>1,2</sup>, Yu-Xian Zhang<sup>1,2</sup>, Wen-Huai  
4 Song<sup>1,2</sup>, Yu-Chi Lin<sup>1,2</sup>, Yan-Lin Zhang<sup>1,2\*</sup>

5 <sup>1</sup>. School of Ecology and Applied Meteorology and Atmospheric Environment Center,  
6 Joint Laboratory for International Cooperation on Climate and Environmental Change,  
7 Ministry of Education, Nanjing University of Information Science & Technology,  
8 Nanjing 210044, China.

9 <sup>2</sup>. Jiangsu Key Laboratory of Atmospheric Environment Monitoring and Pollution  
10 Control, Collaborative Innovation Center on Forecast and Evaluation of  
11 Meteorological Disasters (CIC-FEMD), Nanjing University of Information Science &  
12 Technology, Nanjing 210044, China.

13

14 **\*Correspondence:** Yan-Lin Zhang ([dryanlinzhang@outlook.com](mailto:dryanlinzhang@outlook.com))

15

16 **Abstract.** Atmospheric low molecular weight amines play important roles in aerosol  
17 physiochemical properties and climate. However, the compositions, sources, and  
18 secondary formation mechanisms of amines in offshore aerosols remain unclear. Here,  
19 an integrated observation of methylamine (MA), ethylamine (EA), dimethylamine  
20 (DMA), iso-propanamine (IPA), propanamine (PA), “trimethylamine + diethylamine”  
21 (TMDEA), and over 100 other chemical components was conducted in total  
22 suspended particles samples collected during a spring 2018 research cruise across the  
23 Yellow Sea and Bohai Sea, China. Concentrations of total amines exhibited a  
24 north-to-south decrease from the Bohai Sea to the South Yellow Sea, corresponding to  
25 the decreasing influence of terrestrial air masses. Source analyses of amines were  
26 performed using specific organic molecular tracers representing primary biogenic  
27 sources, higher plant waxes, marine/microbial sources, biogenic secondary organic  
28 aerosols, biomass burning, and fossil fuel combustion, and two major secondary  
29 formation pathways were inferred. MA, EA, and DMA were largely influenced by  
30 terrestrial biogenic and anthropogenic sources, with the majority (74.0%, 52.6%, and  
31 65.7%) formed via nitrate-associated secondary formation pathways. PA was mainly  
32 derived from combustion-related sources along with terrestrial and marine biogenic  
33 contributions. In contrast, the predominant TMDEA was mostly generated via  
34 sulfate-associated secondary formation pathways (61.8%) and contributed by marine  
35 emissions, resulting in spatial pattern distinct from other major amines and the  
36 north-to-south increasing relative contributions of amines in aerosols. These results  
37 highlight the impact of terrestrial emissions on offshore aerosol chemistry and the  
38 importance of origins and multiphase chemistry of amines under varying ambient  
39 conditions.

40

## 41 **1 Introduction**

42 Amines, derivatives of ammonia (NH<sub>3</sub>) with one or more hydrogen atoms replaced by  
43 alkyl or aryl groups, represent an important class of nitrogen-containing organic  
44 compounds (Shen et al., 2023; Zhu et al., 2022; Liu et al., 2023). Low molecular  
45 weight amines, such as methylamine (MA), dimethylamine (DMA), trimethylamine  
46 (TMA), ethylamine (EA), diethylamine (DEA), and propanamine (PA), are the most  
47 common and abundant atmospheric amines. They are ubiquitous in both the gas and  
48 particle phases due to high water solubility and strong alkalinity (Ge et al., 2011b, a).  
49 These amines are primarily emitted in the gas phase and mainly occur in aerosols as  
50 aminium salts formed via chemically reactive gas-to-particle conversion, commonly  
51 referred to as secondary formation of amines.

52 Gaseous amines can be oxidized by atmospheric oxidants (including OH, O<sub>3</sub>, and NO<sub>x</sub>)  
53 (Tang et al., 2013; Nielsen et al., 2012), and undergo gas-to-particle conversion  
54 through direct dissolution (Liu et al., 2018), acid-base reactions (Liu et al., 2023;  
55 Barsanti and Pankow, 2006; Chen et al., 2022), and heterogeneous reactions (Pankow,  
56 2015; Chan and Chan, 2013; Qiu and Zhang, 2013), leading to the formation of  
57 secondary organic aerosols (SOA) that aggravate air quality and visibility. Gaseous  
58 amines and their oxidization products, such as nitrosamines, pose significant risks to  
59 human health (Li et al., 2019a; Lee and Wexler, 2013). The multiphase chemistry of  
60 atmospheric amines participates in and accelerates new particle formation (Liu et al.,  
61 2022; Huang et al., 2022; Yao et al., 2018; Shen et al., 2019), enhances aerosol  
62 hygroscopicity (Chu et al., 2015; Gomez-Hernandez et al., 2016), and promotes the  
63 activation of cloud condensation nuclei (Tang et al., 2014; Corral et al., 2022;  
64 Gomez-Hernandez et al., 2016). Additionally, amines can promote the formation of  
65 brown carbon (Marrero-Ortiz et al., 2018; Lin et al., 2015), thereby affecting

66 atmospheric radiation and climate. However, challenges in detecting minute levels of  
67 amines, the scarcity of ambient measurements, and a limited process-based  
68 understanding of aerosol formation have led to the underrepresented of amines in  
69 global climate models (Kanawade and Jokinen, 2025).

70 Atmospheric amines originate from diverse natural sources (e.g. ocean, soil, and  
71 vegetation) and anthropogenic sources (e.g. animal husbandry, biomass burning, coal  
72 combustion, vehicle emissions, composting, waste incineration, industrial activities,  
73 and sewage) (Shen et al., 2017; Hemmilä et al., 2018; Feng et al., 2022). The ocean is  
74 an important natural source of low molecular weight amines, with emissions mainly  
75 driven by biological processes (Calderón et al., 2007; Wang and Lee, 1994). Global  
76 modeling (Myriokefalitakis et al., 2010) suggested that amines contribute ~20% of  
77 marine SOA, ranking second to dimethylsulfide (DMS). However, this contribution  
78 may be substantially overestimated, given that the actual proportions of amines  
79 relative to  $\text{NH}_3$  are up to three orders of magnitude lower than the values assumed in  
80 the model. Measured concentrations of amines varying across different oceans in both  
81 seawater and the atmosphere (Violaki and Mihalopoulos, 2010; Gibb et al., 1999; Van  
82 Neste et al., 1987). Elevated concentrations of DMA and TMA are associated with  
83 marine biological activities (Carpenter et al., 2012; Welsh, 2000) and algal blooms  
84 (Müller et al., 2009; Facchini et al., 2008b). Marine organisms act as both sources and  
85 sinks of amines, and the source/sink capability of the ocean varies with ambient  
86 conditions (Pinxteren et al., 2019). For instance, TMA can be released from living  
87 tissues or during biodegradation and decay, and can also be utilized by  
88 microorganisms for energy metabolism (Sun et al., 2019; Köllner et al., 2017; Lidbury  
89 et al., 2015). TMA can be biologically oxidized to trimethylamine oxide (TMAO), an  
90 osmotic regulatory compound in marine organisms and a precursor of DMA and MA

91 (Chen et al., 2011; Lidbury et al., 2017). The calculated sea-to-air fluxes of DMA at  
92 Cape Verde were both positive and negative, whereas those of MA were mostly  
93 positive (Pinxteren et al., 2019). Amines in marine aerosols can originate from sea  
94 spray (Bates et al., 2012; Gorzelska and Galloway, 1990), bubble bursting (Milne and  
95 Zika, 1993), and gas-to-particle conversion, i.e. secondary formation (Rinaldi et al.,  
96 2010; Facchini et al., 2008b; Facchini et al., 2008a). Most low molecular weight  
97 amines in marine aerosols were considered to be secondarily formed (Gaston et al.,  
98 2013; Dall'osto et al., 2019). For instance, 11–25% of MA, DMA and TMA in the  
99 Antarctic sympagic environment originated from primary marine aerosols, whereas  
100 75–89% were incorporated into aerosols after air-sea exchange (Dall'osto et al., 2019).  
101 Amines in marine aerosols may also be influenced by inland sources and long-range  
102 atmospheric transportation (Nielsen et al., 2012). TMA detected in aerosols off the  
103 coast of California was associated with inland animal husbandry activities rather than  
104 local marine biogenic emissions (Gaston et al., 2013).

105 Atmospheric low molecular weight amines have been widely reported in urban  
106 (Cheng et al., 2020; Chen et al., 2019; Liu et al., 2017), rural (Cheng et al., 2018; Lin  
107 et al., 2017), and coastal areas (Liu et al., 2022; Hu et al., 2015; Zhou et al., 2019; Du  
108 et al., 2021), but relatively few studies have focused on marine regions of China  
109 (Zhou et al., 2019; Yu et al., 2016; Hu et al., 2015). The Yellow Sea (YS) and Bohai  
110 Sea (BS) are two marginal seas in eastern China that serve as transition zones for  
111 atmospheric pollutants and particles transported from East Asia to the Northwest  
112 Pacific Ocean (NWPO). The YS is divided into South Yellow Sea (SYS) and North  
113 Yellow Sea (NYS), both semi-open sea areas of the NWPO. The BS is the  
114 northernmost marginal sea of China, surrounded by land on three sides and bordered  
115 to the east by the NYS. Aerosols over the YS–BS are significantly influenced by the

116 transportation of terrestrial emissions from northern and eastern China during the  
117 prevailing spring East Asia monsoon (Fang et al., 2016). Previous studies on aerosol  
118 amines over the marginal seas of China have mainly focused on DMA and TMDEA,  
119 the sum of TMA and DEA (Zhou et al., 2019; Xie et al., 2018; Yu et al., 2016; Hu et  
120 al., 2015). Although MA has been observed as the dominant amine in urban aerosols  
121 in northern China and the Yangtze River Delta region (Yang et al., 2023; Liu et al.,  
122 2023; Huang et al., 2018), its contribution in marine aerosols of China remains  
123 unclear. The primary sources and secondary formation pathways of aerosol amines  
124 over the YS–BS are poorly constrained due to the combined influence of complex  
125 terrestrial and marine emissions, as well as the lack of specific source indicators. To  
126 address these, an integrated analysis of six major amines together with more than 100  
127 other chemical components in aerosols was conducted using filter samples collected  
128 over the YS–BS during a research cruise in spring 2018. Spatial variations, potential  
129 sources, and secondary formation pathways of aerosol amines were investigated. By  
130 elucidating the relationships between individual amines and specific organic  
131 molecular tracers representing six source categories, this study provides new  
132 observational constraints on the sources and atmospheric processing of amines in  
133 marine aerosols. The results suggest that individual amines were associated with  
134 different primary sources and likely underwent two distinct major secondary  
135 formation pathways. These findings provide a basis for improving the quantitative  
136 source apportionment of aerosol amines and for further clarify their origins and  
137 gas-to-particle conversion under varying ambient conditions.

## 138 **2 Methods**

### 139 **2.1 Aerosol sampling**

140 During a Chinese oceanographic cruise over the YS–BS (28 March–16 April 2018),  
141 total suspended particles (TSP) samples were collected on prebaked (450 °C for 6 h)  
142 quartz fiber filters using a high-volume air sampler (ASM-1000, Guangzhou; flow  
143 rate: 1 m<sup>3</sup> min<sup>-1</sup>) aboard the *Dong Fang Hong 2* (Figure S1 and Table S1). The  
144 sampler was installed windward on the upper deck at the ship bow (~10 m above the  
145 sea surface). To avoid contamination from the ship exhaust, sampling was performed  
146 only while the vessel was underway. During the sampling period, a total of 15  
147 samples were collected, and 3 field blank filters were prepared by collecting without  
148 airflow. The samples were categorized into SYS, NYS, and BS by sampling positions.  
149 Real-time navigation and meteorological data, including position (longitude and  
150 latitude), ambient temperature (T), relative humidity (RH), and wind speed, were  
151 recorded by the onboard monitoring system.

152

### 153 **2.2 Chemical analysis**

154 Low molecular weight amines can be directly separated and quantified using ion  
155 chromatography methods (Feng et al., 2020; Place et al., 2017; VandenBoer et al.,  
156 2012). Six major protonated amine species extracted from TSP filter samples,  
157 including methylamine (CH<sub>3</sub>NH<sub>3</sub><sup>+</sup>, MA), ethylamine (CH<sub>3</sub>CH<sub>2</sub>NH<sub>3</sub><sup>+</sup>, EA),  
158 dimethylamine [(CH<sub>3</sub>)<sub>2</sub>NH<sub>2</sub><sup>+</sup>, DMA], iso-propanamine [(CH<sub>3</sub>)<sub>2</sub>CHNH<sub>3</sub><sup>+</sup>, IPA],  
159 propanamine (CH<sub>3</sub>CH<sub>2</sub>CH<sub>2</sub>NH<sub>3</sub><sup>+</sup>, PA), and the combined species “trimethylamine  
160 [(CH<sub>3</sub>)<sub>3</sub>NH<sup>+</sup>, TMA] + diethylamine [(CH<sub>3</sub>CH<sub>2</sub>)<sub>2</sub>NH<sub>2</sub><sup>+</sup>, DEA]” (TMDEA), were  
161 measured by a Thermo Fisher Scientific Dionex ICS-5000+ system, as described in

162 detail elsewhere (Yang et al., 2023). Before analysis, a 0.8 cm<sup>2</sup> portion of each sample  
163 or blank filter was ultrasonically extracted 3 times with 10–30 mL of ultrapure water  
164 for 15 min in an ice-water bath, followed by filtration through a 0.22 μm Teflon filter.  
165 The analytical precision was better than 10%, and recoveries for all amines ranged  
166 from 90% to 110%. The method detection limits (MDLs) for MA, EA, DMA, IPA, PA,  
167 and TMDEA were 0.4 ng m<sup>-3</sup>, 0.4 ng m<sup>-3</sup>, 0.5 ng m<sup>-3</sup>, 0.7 ng m<sup>-3</sup>, 1.1 ng m<sup>-3</sup>, and 2.9  
168 ng m<sup>-3</sup>, respectively.

169 To provide a comprehensive characterization, other key chemical components in TSP  
170 samples were also analyzed, including water-soluble inorganic ions (WSIIs; Na<sup>+</sup>,  
171 NH<sub>4</sub><sup>+</sup>, K<sup>+</sup>, Mg<sup>2+</sup>, Ca<sup>2+</sup>, Cl<sup>-</sup>, NO<sub>3</sub><sup>-</sup>, SO<sub>4</sub><sup>2-</sup>, etc.), low molecular weight organic acids  
172 (CHO<sub>2</sub><sup>-</sup>, C<sub>2</sub>H<sub>3</sub>O<sub>2</sub><sup>-</sup>, C<sub>4</sub>H<sub>4</sub>O<sub>4</sub><sup>2-</sup>, C<sub>5</sub>H<sub>6</sub>O<sub>4</sub><sup>2-</sup>, CH<sub>3</sub>O<sub>3</sub>S<sup>-</sup>/MSA<sup>-</sup>, etc.), carbonaceous  
173 components (TC, OC, and EC), and organic compositions (polar and nonpolar).  
174 Detailed methodologies had been described elsewhere (Fan et al., 2019; Cao et al.,  
175 2024), and the measurement results were summarized in Table S2.

176

### 177 **2.3 Auxiliary data**

178 Average chlorophyll *a* (Chl *a*) concentrations in seawater during the sampling period  
179 were retrieved from combined Aqua-MODIS and Terra-MODIS datasets  
180 (<https://oceancolor.gsfc.nasa.gov/>) using ArcGIS software (Figure S2). Fire spot  
181 information was obtained from the Fire Information for Resource Management  
182 System (FIRMS, <https://firms.modaps.eosdis.nasa.gov/>). Based on the archived  
183 Global Data Assimilation System (<ftp://arlftp.arlhq.noaa.gov/pub/archives/gdas1/>)  
184 meteorological data, 48 h backward air-mass trajectories at 200 m above ground level  
185 were calculated using the Hybrid Single-particle Lagrangian Integrated Trajectory

186 (HYSPLIT) model, and subsequently processed with MeteoInfo software (Figure S3).  
187 The trajectories were calculated from the position and time point at the beginning of  
188 each sampling, with hourly intervals thereafter.

189

## 190 **3 Results and discussion**

### 191 **3.1 Overview of amines in marine aerosols**

192 During the research cruise over the YS–BS from 28 March to 16 April 2018, total  
193 concentrations of MA, EA, DMA, IPA, PA, and TMDEA ( $\Sigma$ amines) in TSP ranged  
194 from 16.2 ng m<sup>-3</sup> to 89.1 ng m<sup>-3</sup> (Figure 1). Lower  $\Sigma$ amines concentrations were  
195 observed over the SYS and NYS, averaging 40.4 ± 16.4 ng m<sup>-3</sup> and 43.5 ± 17.5 ng  
196 m<sup>-3</sup>, respectively, and higher concentrations occurred over the BS, averaging 63.6 ±  
197 18.3 ng m<sup>-3</sup>. Concentrations of other chemical components, including total WSIs, TC,  
198 and total measured organic compositions, exhibited a similar spatial pattern (SYS <  
199 NYS < BS; Table S2).

200 TMDEA was the predominant amine species in TSP over the YS–BS, with  
201 concentrations ranging from 6.1 ng m<sup>-3</sup> to 36.3 ng m<sup>-3</sup> (Figure S4) and averages of  
202 20.7 ± 9.1 ng m<sup>-3</sup>, 17.8 ± 7.3 ng m<sup>-3</sup>, and 23.8 ± 3.7 ng m<sup>-3</sup> over the SYS, NYS, and  
203 BS, respectively. The fraction of TMDEA in  $\Sigma$ amines decreased from the SYS  
204 (51.2%) to the NYS (40.8%) and BS (37.4%). The concentrations of amines measured  
205 in TSP were comparable to PM<sub>2.5</sub> and PM<sub>10</sub> (Table S3), as amines are predominantly (>  
206 70%) distributed in aerosols with diameters < 1.8 μm (Zhou et al., 2019; Xie et al.,  
207 2018; Yu et al., 2016). Compared with other marine and coastal regions, the aerosol  
208 TMDEA concentrations in spring over the YS–BS were higher than those reported for  
209 the East China Sea (ECS), Huaniao Island (in the ECS), South China Sea (SCS), and

210 Northwest Pacific Ocean (NWPO) (Chen et al., 2022; Zhou et al., 2019; Xie et al.,  
211 2018; Yu et al., 2016). Over the YS–BS, aerosol TMDEA concentrations were higher  
212 in summer than in spring and autumn (Xie et al., 2018; Yu et al., 2016).

213 MA, the second most abundant amine species (range: 0.9–44.0 ng m<sup>-3</sup>), exhibited  
214 average concentrations of 22.8 ± 15.0 ng m<sup>-3</sup> and 15.7 ± 7.7 ng m<sup>-3</sup> in TSP over the  
215 BS and NYS, contributing 35.9% to ∑amines. Relatively lower MA concentrations  
216 (10.0 ± 7.0 ng m<sup>-3</sup>) and a smaller proportion of MA to ∑amines (24.9%) were  
217 observed over the SYS compared with the NYS–BS. A markedly high MA  
218 concentration was found in S14, the cruise track of which was close to land and  
219 largely influenced by terrestrial air masses (Figure S3 and Figure S4). The average  
220 aerosol MA concentration over the YS–BS in spring (13.7 ng m<sup>-3</sup>) was comparable to  
221 that at Jeju Island, South Korea (Yang et al., 2004), and was higher than those at  
222 coastal Qingdao (a port city surrounded by the YS and BS) and Huaniao Island in  
223 winter (Liu et al., 2022; Huang et al., 2018). These values were further higher than  
224 those reported for the Arabian Sea (Gibb et al., 1999) and tropical Atlantic (Pinxteren  
225 et al., 2019), where measurements focused on ultrafine particles may underestimate  
226 aerosol amines concentrations to some extent.

227 DMA concentrations ranged from 1.3 ng m<sup>-3</sup> to 10.4 ng m<sup>-3</sup>, with averages of 3.5 ±  
228 2.1 ng m<sup>-3</sup>, 3.8 ± 2.6 ng m<sup>-3</sup>, and 7.9 ± 2.1 ng m<sup>-3</sup> in TSP over the SYS, NYS, and BS,  
229 respectively. Higher DMA contributions to ∑amines were found over the BS (12.4%)  
230 than the NYS (8.7%) and SYS (8.6%). The average aerosol DMA concentration over  
231 the YS–BS in spring (4.4 ng m<sup>-3</sup>) was much lower than those reported for coastal  
232 Qingdao in winter and for the YS–BS in different seasons in previous years (Table  
233 S3). EA (0.6–4.8 ng m<sup>-3</sup>), IPA (0.5–3.9 ng m<sup>-3</sup>), and PA (1.3–5.1 ng m<sup>-3</sup>) constituted  
234 a relatively small fraction of ∑amines (7.3–28.2%), with average concentrations of

235  $2.0 \pm 1.2 \text{ ng m}^{-3}$ ,  $1.8 \pm 1.0 \text{ ng m}^{-3}$ , and  $2.9 \pm 1.0 \text{ ng m}^{-3}$  in TSP over the YS–BS,  
236 respectively. The average aerosol EA concentration over the BS ( $3.0 \text{ ng m}^{-3}$ ) was  
237 comparable to those observed at coastal Qingdao (Liu et al., 2022) and Jeju Island,  
238 South Korea (Yang et al., 2004). Comparable data for EA, IPA, and PA concentrations  
239 in marine aerosols were currently limited.

240 According to air-mass analyses (Figure S3), S3 and S12–19 (include all samples from  
241 the NYS–BS) were strongly influenced by continental outflow, while S5, S6, and S8  
242 (from the SYS) were dominated by marine air masses. The remaining samples were  
243 affected by mixed terrestrial and marine air masses. Higher concentrations of MA  
244 ( $16.0 \pm 11.5 \text{ ng m}^{-3}$ ), EA ( $2.3 \pm 1.4 \text{ ng m}^{-3}$ ), DMA ( $5.3 \pm 2.9 \text{ ng m}^{-3}$ ), and PA ( $3.2 \pm$   
245  $1.0 \text{ ng m}^{-3}$ ) were observed in samples influenced by continental outflow compared to  
246 those dominated by marine air masses (MA:  $10.0 \pm 6.6 \text{ ng m}^{-3}$ ; EA:  $1.3 \pm 0.2 \text{ ng m}^{-3}$ ;  
247 DMA:  $2.0 \pm 0.1 \text{ ng m}^{-3}$ ; and PA:  $2.3 \pm 1.0 \text{ ng m}^{-3}$ ). In contrast, TMDEA  
248 concentrations were higher in samples dominated by marine air masses ( $27.6 \pm 9.1 \text{ ng}$   
249  $\text{m}^{-3}$ ) than those influenced by continental outflow ( $19.8 \pm 7.4 \text{ ng m}^{-3}$ ). Strong positive  
250 correlations were observed among MA, EA, and DMA ( $R = 0.73\text{--}0.77$ ,  $P < 0.01$ ),  
251 whereas no statistically significant correlation ( $P > 0.05$ ) exhibited between IPA, PA,  
252 or TMDEA and other amine species. These results suggested that MA, EA, and DMA  
253 might share similar sources and secondary formation pathways, whereas IPA, PA, and  
254 TMDEA were likely influenced by different sources or atmospheric processes.

255

### 256 **3.2 Relative contributions of amines in TSP over the YS–BS**

257 Amines, as a subset of water-soluble organic carbon, generally constitute only a minor  
258 fraction of OC. Both OC and EC concentrations in TSP increased from the SYS to the

259 NYS and BS (Figure 2), consistent with the strengthened influence of atmospheric  
260 pollutants transported from mainland East Asia (Figure S3). However, the  
261  $\sum$ amines-C/OC ratios (2.1–8.8‰) were relatively higher in aerosols over the SYS (5.4  
262  $\pm$  2.2‰) than the NYS (4.4  $\pm$  1.7‰) and BS (4.0  $\pm$  1.4‰; Figure S5), contrary to the  
263 spatial variation of  $\sum$ amines concentrations.

264 Positive correlations were found between  $\text{NH}_4^+$  and amines, including MA (R = 0.78,  
265 P < 0.01), DMA (R = 0.74, P < 0.01), EA (R = 0.57, P < 0.05), PA (R = 0.58, P < 0.05),  
266 and TMDEA (R = 0.52, P < 0.05). Aerosol  $\text{NH}_4^+$  is formed via the heterogeneous  
267 uptake of  $\text{NH}_3$ , the most abundant alkaline gas in the atmosphere, by acidic aerosols,  
268 and exists as ammonium sulfate  $[(\text{NH}_4)_2\text{SO}_4]$ , ammonium bisulfate ( $\text{NH}_4\text{HSO}_4$ ),  
269 ammonium nitrate ( $\text{NH}_4\text{NO}_3$ ), and ammonium chloride ( $\text{NH}_4\text{Cl}$ ) (Behera et al., 2013).  
270 Atmosphere  $\text{NH}_3$  shares overlapping source profiles with gaseous amines, including  
271 animal husbandry, biomass burning, vehicle emissions, industrial activities, soil, and  
272 the ocean. This was inferred as the reason for observed correlations between  $\text{NH}_4^+$   
273 and amines in aerosols.

274 Gaseous low molecular weight amines are more alkaline than  $\text{NH}_3$ , and may compete  
275 with  $\text{NH}_3$  in atmospheric acid-base reactions (Sorooshian et al., 2008; Chen et al.,  
276 2022). The molar ratios of aerosol amines to  $\text{NH}_4^+$  were calculated to assess their  
277 relative contributions to the neutralization of acidic species in aerosols (Hu et al.,  
278 2015). The  $\sum$ amines/ $\text{NH}_4^+$  molar ratios (4.8–17.0‰) were 9.7  $\pm$  3.4‰, 7.6  $\pm$  0.8‰,  
279 and 6.8  $\pm$  1.8‰ over the SYS, NYS, and BS, respectively. The spatial pattern of  
280  $\sum$ amines/ $\text{NH}_4^+$  molar ratios (SYS > NYS > BS) was consistent with that of the  
281  $\sum$ amines-C/OC ratios, both indicating a north-to-south increase in the relative  
282 contributions of amines to aerosol composition over the YS–BS.

283 The  $\sum$ amines/ $\text{NH}_4^+$  molar ratios obtained in this study were of the same order of

284 magnitude as those reported previously (Xie et al., 2018; Yu et al., 2016). Overall,  
285 amines contribute negligibly to the neutralization of acidic species in TSP compared  
286 with  $\text{NH}_4^+$ , which is reasonable given the much higher atmospheric abundance of  $\text{NH}_3$   
287 relative to gaseous amines (Zheng et al., 2015; You et al., 2014; Ge et al., 2011b, a).  
288 However, amines potentially play a more important role in neutralizing acidic species  
289 in submicron particles, particularly in the presence of organic compounds (Xie et al.,  
290 2018). The composition of  $\text{NH}_4^+$ ,  $\text{NO}_3^-$ , and  $\text{SO}_4^{2-}$  may influence aerosol amines, as  
291 they can act as competitors for neutralization and as major reactants in aerosol  
292 formation. The  $\text{NH}_4^+ / (\text{Cl}^- + \text{NO}_3^- + 2 \times \text{SO}_4^{2-})$  molar ratios is commonly used to  
293 assess whether  $\text{NH}_4^+$  fully neutralizes acidic species ( $\text{Cl}^-$ ,  $\text{NO}_3^-$ , and  $\text{SO}_4^{2-}$ ) in  
294 aerosols. In this study, the ratios in TSP over the YS–BS were mostly  $< 1$  ( $0.8 \pm 0.2$ ;  
295 Figure 2 and Figure S5), indicating  $\text{NH}_4^+$  deficiency. This deficiency was more  
296 markedly over the BS ( $0.6 \pm 0.0$ ) than the YS ( $0.8 \pm 0.2$ ). The  $\text{NO}_3^- / \text{SO}_4^{2-}$  molar  
297 ratios in TSP over the SYS ( $0.8 \pm 0.8$ ) were significantly lower than those over the  
298 NYS ( $2.3 \pm 0.4$ ) and BS ( $2.5 \pm 0.8$ ), indicating that  $\text{SO}_4^{2-}$  was the dominate acidic  
299 species in SYS aerosols, whereas  $\text{NO}_3^-$  dominated in NYS and BS aerosols. The  
300 composition of  $\text{NH}_4^+$ ,  $\text{NO}_3^-$ , and  $\text{SO}_4^{2-}$  in NYS aerosols was intermediate between  
301 that over the BS and SYS, consistent with the regional variations in amines  
302 concentrations and composition. Molar concentrations of  $\sum$ amines increased with  
303 increasing  $\text{NH}_4^+$  deficiency [indicated by  $\text{NH}_4^+ / (\text{Cl}^- + \text{NO}_3^- + 2 \times \text{SO}_4^{2-})$  molar ratios;  
304  $R = -0.57$ ,  $P < 0.05$ ] and with  $\text{NO}_3^- / \text{SO}_4^{2-}$  ratios ( $R = 0.56$ ,  $P < 0.05$ ), particularly in  
305 BS aerosols. Nevertheless, individual amines responded differently to variations in  
306  $\text{NH}_4^+$  deficiency and  $\text{NO}_3^- / \text{SO}_4^{2-}$  molar ratios, likely reflecting differences in their  
307 primary sources (terrestrial vs. marine) and formation pathways (nitrate vs. sulfate  
308 associated).

### 310 3.3 Source analysis of amines in TSP over the YS–BS

#### 311 3.3.1 Biogenic sources

312 On a global scale, the ocean is a major source of gaseous methylamines (fluxes: TMA >  
313 MA >> DMA) (Van Neste et al., 1987; Schade and Crutzen, 1995). Intensive ocean  
314 farming is widespread in the coastal areas of the YS–BS (Hu et al., 2015), where  
315 marine biogenic sources, including fish emission (Namieśnik et al., 2003),  
316 biodegradation of nitrogen-containing materials, and decay process (Calderón et al.,  
317 2007) may release gaseous amines into the atmosphere. The concentration of Chl *a* in  
318 surface seawater is an indicator of phytoplankton biomass and thus reflects the  
319 intensity of marine biogenic emissions to some extent. Significantly higher Chl *a*  
320 concentrations were observed in the BS than in the YS, with relatively elevated values  
321 in near shore areas (Figure S2). The spatial distribution of  $\Sigma$ amines in TSP over the  
322 YS–BS was broadly consistent with, though not identical to, Chl *a* concentrations in  
323 surface seawater. This discrepancy likely reflected secondary formation of amines in  
324 aerosols, as well as the influence of long-range transportation of terrestrial emissions  
325 driven by the prevailing East Asia monsoon during spring, particularly to S3 and  
326 S12–19 (Figure S3).

327 Aerosol MA, EA, and DMA exhibited positive linear relationships with total primary  
328 sugars and sugar alcohols (Figure 3 a–c and Table S4), which mainly originate from  
329 primary biogenic sources such as bacteria, pollen, and plant or animal debris (Li et al.,  
330 2019b). These sources can be either marine or terrestrial. Fungal spore OC and plant  
331 debris OC were estimated from mannitol and arabitol (Bauer et al., 2008), and glucose  
332 (Zheng et al., 2018), respectively. Significant positive correlations were observed

333 between MA, EA, and DMA and fungal spore OC, plant debris OC, and several  
334 individual primary sugars and sugar alcohols (e.g., trehalose,  $\alpha$ -fructose, and sucrose;  
335  $R > 0.50$ ,  $P < 0.05$ ). DMA exhibited the strongest correlation with trehalose ( $R = 0.71$ ,  
336  $P < 0.01$ ), a compound abundant in microorganisms, algae, plants, and invertebrates,  
337 and also acts as an indicator of re-suspended dust (Medeiros et al., 2006; Simoneit et  
338 al., 2004). In addition, MA, DMA, and PA were positively correlated with high  
339 molecular weight *n*-alkanes ( $ALK_{HMW}$ ;  $C_{27}$ ,  $C_{29}$ ,  $C_{31}$  and  $C_{33}$ ) and fatty alcohols  
340 ( $ALC_{HMW}$ ;  $> C_{19alc}$ ; Figure 3 d–e), while PA also correlated with low molecular  
341 weight fatty acids ( $FA_{LMW}$ ;  $\leq C_{19:0}$ ; Figure 3 f).  $ALK_{HMW}$  (Rogge et al., 1993),  
342  $ALC_{HMW}$  (Simoneit et al., 1991), and high molecular weight fatty acids ( $FA_{HMW}$ ;  $>$   
343  $C_{19:0}$ ) are tracers of higher plant waxes from terrestrial vegetation, whereas  $FA_{LMW}$  are  
344 associated with marine/microbial sources (Haque et al., 2019). Overall, these results  
345 indicated that amines (MA, EA, DMA, and PA) in TSP over the YS–BS were  
346 contributed by biogenic sources. MA and DMA were largely influenced by terrestrial  
347 biogenic emissions, whereas PA was affected by both terrestrial and marine biogenic  
348 sources.

349 Atmospheric biogenic secondary organic aerosols (BSOA) are formed via the  
350 photochemical oxidation of biogenic volatile organic compounds (BVOCs) by  $O_3$ ,  
351 OH and  $NO_x$  (Ng et al., 2011). In this study, six isoprene SOA ( $SOA_I$ ) tracers, three  
352 monoterpene SOA ( $SOA_M$ ) tracers, and one  $\beta$ -caryophyllene SOA ( $SOA_C$ ) tracer were  
353 measured in TSP over the YS–BS. Biogenic SOC derived from isoprene,  
354 monoterpene, and  $\beta$ -caryophyllene was estimated using the tracer-based method  
355 (Kang et al., 2018; Kleindienst et al., 2007). Significant positive linearity were  
356 observed between MA and both isoprene and monoterpene SOC (Figure 3 g–h).  
357 Among the  $SOA_I$  tracers, MA exhibited stronger correlations with 2-methyltetrols

358 (2-MTLs;  $R = 0.74$ ,  $P < 0.01$ ) and  $C_5$ -alkene triols ( $R = 0.66$ ,  $P < 0.01$ ) than with  
359 2-methylglyceric acid (2-MGA;  $R = 0.64$ ,  $P < 0.05$ ). DMA was also positively  
360 correlated with isoprene SOC ( $R = 0.55$ ,  $P < 0.05$ ), only driven by its association with  
361 2-MTLs ( $R = 0.59$ ,  $P < 0.05$ ). Among the  $SOA_M$  tracers, pinonic acid correlated with  
362 MA ( $R = 0.73$ ,  $P < 0.01$ ), EA ( $R = 0.52$ ,  $P < 0.05$ ), and DMA ( $R = 0.58$ ,  $P < 0.05$ ),  
363 while pinic acid only correlated with MA ( $R = 0.59$ ,  $P < 0.05$ ). In addition, PA showed  
364 a positive linearity with  $\beta$ -caryophyllene SOC ( $R = 0.67$ ,  $P < 0.01$ ; Figure 3 i). These  
365 findings supported that MA, EA, DMA, and PA shared common sources with BVOCs  
366 and/or interacted with BSOA formation processes. High concentrations of amines and  
367 biomarkers were simultaneously observed in aerosols over the BS and NYS, whereas  
368 amines in the SYS aerosols remained at moderate levels despite low tracers  
369 concentrations (Figure 3). These indicated that terrestrial biogenic emissions  
370 contributed more substantially to aerosol amines over the BS and NYS than the SYS.

371

### 372 **3.3.2 Anthropogenic sources**

373 Anthropogenic sources are another important contributor to atmospheric amines and  
374 can be broadly categorized into combustion-related sources (e.g., biomass burning,  
375 coal combustion, vehicle emissions, and waste incineration) and non-combustion  
376 sources (e.g., animal husbandry, composting, industrial activities, sewage, and septic  
377 system). EA ( $R = 0.61$ ,  $P < 0.05$ ) and DMA ( $R = 0.72$ ,  $P < 0.01$ ) concentrations in TSP  
378 over the YS–BS increased with EC, indicating the influence of combustion emissions.  
379 Levoglucosan (Lev) is a well-established tracer for biomass burning (Li et al., 2019b).  
380 Concentrations of Lev derived from biomass burning ( $Lev_{bb}$ ) were estimated using  
381 Lev and non-sea-salt  $K^+$  ( $nss-K^+ = K^+ - 0.037 \times Na^+$ ), considering its atmospheric

382 degradation and ~25% non-biomass burning sources [ $Lev_{bb} = 0.75 \times Lev \times$   
383  $nss-K^+ / (0.18 \times Lev + 0.08 \times nss-K^+)$ ]. Biomass burning was not a major source of  
384 MA, EA, and DMA in aerosols over the YS–BS (Figure 3 j), but contributed  
385 substantially to PA, as indicated by the positive linear relationships between PA and  
386 both  $Lev_{bb}$  and lignin products (Figure 3 k–l). The most notable contributor to PA  
387 from biomass burning was conifer burning (the second-largest portion of total  
388 biomass burning) according to the correlations between PA and individual lignin  
389 products, including 4-hydroxybenzoic acid (4-HBA; a herbaceous burning marker and  
390 the predominate lignin product in this study;  $R = 0.52$ ,  $P < 0.05$ ), vanillic acid (VA; a  
391 softwood and hardwood burning marker;  $R = 0.67$ ,  $P < 0.01$ ), syringic acid (SA; also  
392 indicative of softwood and hardwood burning;  $R = 0.60$ ,  $P < 0.05$ ), and  
393 dehydroabietic acid (DA; a conifer burning marker;  $R = 0.71$ ,  $P < 0.01$ ). In addition,  
394 MA ( $R = 0.57$ ,  $P < 0.05$ ) and DMA ( $R = 0.54$ ,  $P < 0.05$ ) were positively correlated  
395 with polycyclic aromatic hydrocarbons (PAHs), indicating potential contributions  
396 from fossil fuel combustion (Table S4). Among all amines, PA showed the strongest  
397 association with combustion-related sources, as evidenced by its correlations with  
398 multiple fossil fuel combustion tracers (Figure 3 m–o), including low molecular  
399 weight n-alkanes ( $ALK_{LMW}$ ;  $C_{20}$ – $C_{26}$ ;  $R = 0.67$ ,  $P < 0.01$ ), PAHs ( $R = 0.63$ ,  $P < 0.05$ ),  
400 hopanes ( $R = 0.55$ ,  $P < 0.05$ ), and steranes ( $R = 0.57$ ,  $P < 0.05$ ).

401 Emissions of amines (MA, DMA, and TMA) from non-combustion anthropogenic  
402 sources, including composting, sewage, and septic systems, are largely linked to  
403 biodegradation process. Therefore, the contribution of non-combustion anthropogenic  
404 sources to amines was encompassed within the primary biogenic sources category.  
405 IPA did not show any correlation with organic molecular tracers in TSP over the  
406 YS–BS. Given its widespread industrial use (e.g., in pesticides, pharmaceuticals, dye

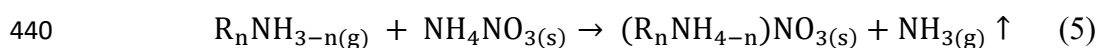
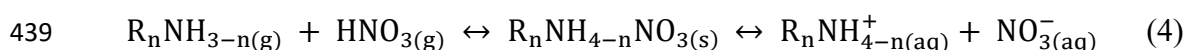
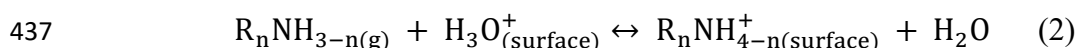
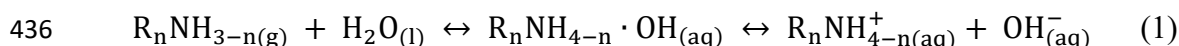
407 intermediates, emulsifiers, detergents, surfactants, and textile additives), aerosol IPA  
408 may be emitted in particulate form from specific industrial activities (Ge et al.,  
409 2011a).

410

### 411 3.3.3 Secondary formation of MA, EA, DMA, and PA

412 Significant correlations were observed between MA, EA, DMA, and PA with  $\text{Cl}^-$  and  
413  $\text{NO}_3^-$  (Figure 4). The regression intercepts of MA, EA, and DMA against  $\text{Cl}^-$  or  $\text{NO}_3^-$   
414 were lower than those with primary organic tracers (Figure 3 and Figure S6),  
415 indicating substantial contributions from secondary formation. The gas-to-particle  
416 conversion of MA, EA, DMA, and PA was inferred to include direct dissolution  
417 (Equation 1), uptake onto acidic particle surfaces (Equation 2) (Yin et al., 2011),  
418 acid-base reactions (Equation 3–4), and displacement reactions with  $\text{NH}_4\text{NO}_3$   
419 (Equation 5) (Bzdek et al., 2010). For MA, EA, and DMA with high water solubility,  
420 direct dissolution is considered as a key step in their gas-to-particle conversion.  
421 Uptake of gaseous amines onto acidic particle surfaces was more important over the  
422 BS, where aerosol acidic species are significantly in excess relative to  $\text{NH}_4^+$ . MA, EA,  
423 DMA, and PA in TSP over the YS–BS were formed via acid-base reactions with  
424 atmospheric HCl and  $\text{HNO}_3$ , while  $\text{CH}_3\text{COOH}$  also contributed to the formation of  
425 aerosol MA, EA and DMA (Figure 4). In TSP over the YS–BS,  $\text{NO}_3^-$  concentrations  
426 were significantly higher than those of  $\text{Cl}^-$  and  $\text{C}_2\text{H}_3\text{O}_2^-$  (Table S2), thus, acid-base  
427 reactions with  $\text{HNO}_3$ , together with displacement reactions involving  $\text{NH}_4\text{NO}_3$ , were  
428 the major pathways for the secondary formation of aerosol MA, EA, DMA and PA.  
429 The partitioning of amines into aerosols was further promoted by low T, high aerosol  
430 acidity, and high RH under dynamic solid/aqueous/gas equilibrium conditions. During

431 the cruise, lower average T were observed over the BS (9.0°C) and NYS (6.7°C) than  
 432 the SYS (9.5°C), and RH remained at a high level across the YS–BS (mean: 86.2%;  
 433 median: 87.6%). The relatively abundant acidic species and lower T over the BS and  
 434 NYS favored the partitioning of MA, EA, DMA, and PA into the particle phase  
 435 compared with the conditions over the SYS.



441 Contributions of nitrate-associated secondary formation to aerosol amines were  
 442 estimated from the average amine concentrations weighted by  $\text{NO}_3^-$  concentrations  
 443 and regression intercepts (Figure S6). These estimates are semi-quantitative and  
 444 limited by the small sample sizes, rather than representing quantitative source  
 445 apportionment or mechanistic yields. Contributions of nitrate-associated secondary  
 446 formation to  $\sum$ amines were highest in TSP over the BS ( $43.0 \pm 26.9\%$ ), followed by  
 447 the NYS ( $33.8 \pm 19.7\%$ ) and SYS ( $21.8 \pm 18.8\%$ ). Among individual amines,  
 448 nitrate-associated secondary formation contributed most to MA ( $74.0 \pm 61.5\%$ ),  
 449 followed by DMA ( $65.7 \pm 44.3\%$ ), EA ( $52.6 \pm 55.0\%$ ), and PA ( $35.1 \pm 22.4\%$ ). PA  
 450 was less contributed by secondary formation, likely because it can be directly emitted  
 451 in particulate form or condense into aerosols after emission due to its relatively higher  
 452 boiling point (47.8°C) compared with MA (−6.3°C), EA (16.6°C), and DMA (7.4°C).

453 The relationships among amines (MA, EA, DMA, and PA), BSOA, and  $\text{NO}_3^-$  in TSP  
 454 over the YS–BS suggested potential interactions among their secondary formation

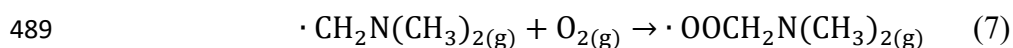
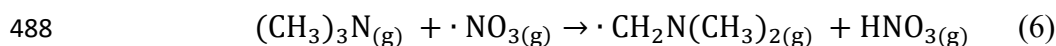
455 processes.  $\text{NO}_x$ , emitted from soil, biogenic activities, and combustion sources, are  
456 important precursors for both BSOA and atmospheric  $\text{HNO}_3$ , which subsequently  
457 forms nitrate aerosols. This was supported by significant positive correlations  
458 between  $\text{NO}_3^-$  and  $\text{SOA}_I$  ( $R = 0.88$ ,  $P < 0.01$ ),  $\text{SOA}_M$  ( $R = 0.86$ ,  $P < 0.01$ ), and  $\text{SOA}_C$   
459 ( $R = 0.64$ ,  $P < 0.05$ ). The formation of MA and DMA in aerosols might occur under  
460 low  $\text{NO}_x$  conditions, as evidenced by their stronger correlations with 2-MTLs or  
461  $\text{C}_5$ -alkene triols (products of isoprene photochemical oxidation under low  $\text{NO}_x$   
462 conditions) (Zheng et al., 2018; Zhang et al., 2011) than with 2-MGA (products of  
463 isoprene aqueous-phase oxidation under high  $\text{NO}_x$  conditions) (He et al., 2018).  
464 Strong atmospheric photo-oxidation generally accelerates the gas-phase degradation  
465 of amines (Lee and Wexler, 2013), thereby reducing the formation of particle-phase  
466 aminium salts. BVOCs, as precursors of BSOA, can generate  $\text{HNO}_3$  via the “ $\text{NO}_3 +$   
467  $\text{HC}$ ” pathway, further promoting the formation of aminium nitrates. Meanwhile,  
468 BSOA formation consumes atmospheric oxidants, which may reduce the degradation  
469 of gaseous amines. The presence of an organic phase also enhances the  
470 competitiveness of amines relative to  $\text{NH}_4^+$  in aerosols (Xie et al., 2018). In addition,  
471 the gas-to-particle conversion of amines may facilitate BSOA formation by providing  
472 more hygroscopic particulate surfaces.

473

#### 474 **3.3.4 Secondary formation of TMDEA**

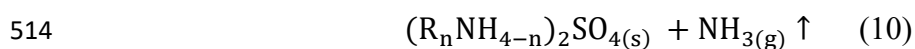
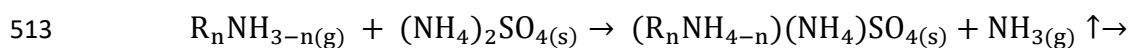
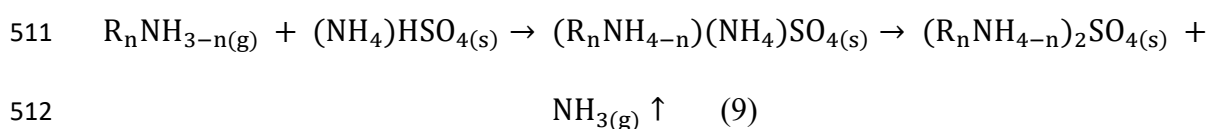
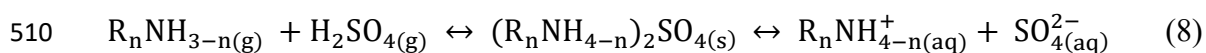
475 Compared with other amines, a larger fraction of TMDEA likely originated from  
476 marine sources, as evidenced by its relatively high concentrations and proportions in  
477 TSP over the SYS, especially in samples dominated by marine air masses. Previous  
478 studies also suggested marine emissions as an important potential source of TMDEA

479 (Schade and Crutzen, 1995; Pinxteren et al., 2019). TMDEA in TSP over the YS–BS  
 480 exhibited no correlation with organic molecular tracers representing primary biogenic  
 481 sources or BSOA (Table S4), although terrestrial vegetation and non-combustion  
 482 anthropogenic sources are also potential sources of gaseous TMDEA (Zhu et al., 2022;  
 483 Ge et al., 2011a). Concentrations of aerosol TMDEA were likely constrained by  
 484 gas-to-particle conversion efficiency. A hypothesis is that part of gaseous TMA  
 485 emitted from primary sources is consumed through reactions with NO<sub>3</sub> to form  
 486 non-aminium-salt SOA (Price et al., 2016; Price et al., 2014) and HNO<sub>3</sub> (Equation 6–  
 487 7).



490 TMDEA in TSP over the YS–BS showed no correlation with Cl<sup>−</sup>, or NO<sub>3</sub><sup>−</sup>, but  
 491 exhibited significant positive linear relationships with SO<sub>4</sub><sup>2−</sup>, C<sub>4</sub>H<sub>4</sub>O<sub>4</sub><sup>2−</sup>, and C<sub>5</sub>H<sub>6</sub>O<sub>4</sub><sup>2−</sup>  
 492 (Figure 4 and Figure S6). The gas-to-particle conversion of TMDEA was inferred to  
 493 include uptake onto acidic particle surfaces (Equation 2), acid-base reactions with  
 494 H<sub>2</sub>SO<sub>4</sub> (Equation 8) and dicarboxylic acids (C<sub>4</sub>H<sub>6</sub>O<sub>4</sub> and C<sub>5</sub>H<sub>8</sub>O<sub>4</sub>), as well as  
 495 displacement reactions with (NH<sub>4</sub>)HSO<sub>4</sub> and (NH<sub>4</sub>)<sub>2</sub>SO<sub>4</sub> (Equation 9–10). Uptake  
 496 onto acidic particle surfaces is considered as a key step in the gas-to-particle  
 497 conversion of TMDEA, as TMA exhibits the strongest alkalinity among gaseous  
 498 amines. TMDEA in TSP over the YS–BS showed limited association with chloride  
 499 and nitrate, likely due to the much lower competitiveness of TMA in forming these  
 500 salts (as reflected by dissociation constants) relative to MA, EA, DMA, and NH<sub>3</sub> (Ge  
 501 et al., 2011b). Instead, acid-base reactions with H<sub>2</sub>SO<sub>4</sub>, together with displacement  
 502 reactions involving (NH<sub>4</sub>)HSO<sub>4</sub> and (NH<sub>4</sub>)<sub>2</sub>SO<sub>4</sub>, were the major pathways for the  
 503 secondary formation of aerosol TMDEA. Contributions of dicarboxylic acids were

504 relatively minor, given the significantly lower concentrations of  $C_4H_4O_4^{2-}$  and  
 505  $C_5H_6O_4^{2-}$  compared with  $SO_4^{2-}$  in TSP over the YS–BS (Table S2). These findings  
 506 were consistent with previous laboratory and theoretical studies showing that TMA  
 507 preferentially reacts with  $H_2SO_4$  (Johnson and Jen, 2023), and that DEA exhibits the  
 508 highest uptake coefficient during the irreversible reactive uptake of gaseous  
 509 ethylamines by  $H_2SO_4$  (Yin et al., 2011).



515 Sulfate-associated secondary formation contributed  $61.8 \pm 31.6\%$  to TMDEA in TSP  
 516 over the YS–BS, as estimated from average TMDEA concentrations weighted by  
 517  $SO_4^{2-}$  concentrations and regression intercept (Figure S6). The contributions were  
 518 highest over the SYS ( $63.4 \pm 36.2\%$ ), followed by the BS ( $61.4 \pm 16.2\%$ ) and NYS  
 519 ( $55.8 \pm 29.3\%$ ). Correspondingly, sulfate-associated secondary formation contributed  
 520  $23.0 \pm 6.0\%$ ,  $22.8 \pm 13.7\%$ , and  $32.5 \pm 22.1\%$  to  $\sum$ amines over the BS, NYS, and  
 521 SYS, respectively. The spatial pattern of average contributions from sulfate-associated  
 522 secondary formation (SYS > BS > NYS) was consistent with that of average T,  
 523 indicating that T conditions influenced the relative advantages of sulfate and nitrate  
 524 formation.

525 Significant positive correlations were observed between non-sea-salt sulfate  
 526 ( $nss-SO_4^{2-} = SO_4^{2-} - 0.2516 \times Na^+$ ) and the dicarboxylates ( $C_4H_4O_4^{2-}$  and  $C_5H_6O_4^{2-}$ ;  
 527  $R = 0.78$  and  $0.66$ ,  $P < 0.01$ ), indicating that these species shared similar potential

528 terrestrial anthropogenic or marine biogenic origins (Miyazaki et al., 2010; Mochida  
529 et al., 2003). Molar concentrations of biogenic-SO<sub>4</sub><sup>2-</sup> were estimated from T and  
530 MSA<sup>-</sup>, as both MSA<sup>-</sup> and SO<sub>4</sub><sup>2-</sup> are oxidation products of DMS emitted from marine  
531 biogenic sources (Nakamura et al., 2005; Bates et al., 1992). Anthropogenic-SO<sub>4</sub><sup>2-</sup>  
532 was then calculated by subtracting biogenic-SO<sub>4</sub><sup>2-</sup> from nss-SO<sub>4</sub><sup>2-</sup>. Biogenic-SO<sub>4</sub><sup>2-</sup>  
533 accounted for 11.1% of total SO<sub>4</sub><sup>2-</sup> in TSP over the SYS, markedly higher than the  
534 NYS (4.3%) and BS (2.1%), yet still representing a minor fraction relative to  
535 anthropogenic-SO<sub>4</sub><sup>2-</sup>. Consequently, TMDEA in TSP over the YS–BS was  
536 predominantly taken up by anthropogenic sulfate aerosols.

537 High concentrations of TMDEA, SO<sub>4</sub><sup>2-</sup>, C<sub>4</sub>H<sub>4</sub>O<sub>4</sub><sup>2-</sup>, and C<sub>5</sub>H<sub>6</sub>O<sub>4</sub><sup>2-</sup> were simultaneously  
538 observed in S5 and S6 over the SYS, along with relatively high marine biogenic  
539 contributions (Biogenic-SO<sub>4</sub><sup>2-</sup>/SO<sub>4</sub><sup>2-</sup>: 11.2% and 10.3%). NH<sub>4</sub><sup>+</sup> deficiency [NH<sub>4</sub><sup>+</sup>/(Cl<sup>-</sup>  
540 + NO<sub>3</sub><sup>-</sup> + 2\*SO<sub>4</sub><sup>2-</sup>): 0.8 and 0.6], high T (12.2°C and 12.1°C), high wind speed (6.9 m  
541 s<sup>-1</sup> and 7.2 m s<sup>-1</sup>), and saturated humidity (RH = 100%) were also found in S5 and S6  
542 (Table S1). Under high RH, more amines partition into aqueous aerosols via direct  
543 dissolution, promoting aminium salts formation, whereas high T shifts the  
544 solid/aqueous/gas equilibrium of aminium salts toward the gas phase. Compared with  
545 the chlorides and nitrates of MA, EA, DMA, and PA, TMDEA sulfates are more  
546 thermally stable. In addition, strong winds enhance the emission of primary marine  
547 aerosols from sea spray and bubble bursting, providing additional amines to TSP, as  
548 amines are present in both seawater and primary marine aerosols. The source  
549 contributions and major secondary formation pathways of amines were summarized in  
550 Figure 5.

551

## 552 **4 Conclusions**

553 This study systematically analyzed the spatial variations, potential sources, and  
554 secondary formation mechanisms of six major low molecular weight amines in  
555 aerosols over the marginal seas of China. Concentrations of total amines, water  
556 soluble inorganic ions, carbonaceous components, and more than 100 organic  
557 compositions generally exhibited a north-to-south decreasing pattern from the BS to  
558 the NYS and SYS. This trend was consistent with the decreasing influence of  
559 continental emissions from mainland East Asia, coupled with the increasing  
560 contribution of the marine atmosphere.

561 Offshore aerosols exhibited distinct compositions of amines compared to terrestrial  
562 aerosols, with TMDEA surpassing MA as the predominant amine. The proportions of  
563 TMDEA in  $\Sigma$ amines and the relative contributions of  $\Sigma$ amines in aerosols increased  
564 from north to south (BS < NYS < SYS), highlighting the ocean as a substantial source  
565 of amines, particularly TMDEA, despite the significant influence of terrestrial  
566 emissions. Distinct potential sources and major secondary formation pathways were  
567 identified for different amine species. MA, EA, and DMA were mainly derived from  
568 terrestrial biogenic and non-combustion anthropogenic sources, followed by fossil  
569 fuel combustion, with over 50% formed via nitrate-associated secondary formation  
570 pathways, interacting with BSOA formation in the  $\text{NO}_x$ -involved oxidation of BVOCs.  
571 In comparison, PA mainly originated from combustion-related sources along with  
572 terrestrial and marine biogenic sources, with only ~35% contributed by  
573 nitrate-associated secondary formation. In contrast to other amines, TMDEA was  
574 mostly (~60%) generated via sulfate-associated secondary formation pathways, and  
575 also contributed by primary marine aerosols from sea spray and bubble bursting.  
576 Terrestrial sources not only emit gaseous amines but also contribute acidic aerosols

577 that can further uptake amines from marine sources during the transportation of air  
578 masses from the mainland to the ocean. This process affects the physiochemical  
579 properties and climate effects of marine aerosols, as well as the carbon and nitrogen  
580 cycles. In addition to precursors abundance, ambient conditions also influence the  
581 secondary formation of aerosol amines, leading to temporal and spatial variations in  
582 their concentrations and compositions. Overall, these findings improve the  
583 understanding of amines in marine aerosols, highlight the impact of terrestrial  
584 emissions on offshore aerosol chemistry, and underscore the importance of multiphase  
585 chemical processes of amines under diverse ambient conditions.

586

587 *Data availability.* Data are available from the corresponding author on request  
588 ([dryanlinzhang@outlook.com](mailto:dryanlinzhang@outlook.com)).

589

590 *Supplement.* The supplement related to this article is available online at: .

591

592 *Author contributions.* Xiao-Ying Yang wrote the draft and produced all the figures and  
593 tables. Fang Cao, Yu-Chi Lin, and Yan-Lin Zhang provided useful comments and  
594 revised the paper. Chang-Liu Wu, Yu-Xian Zhang, and Wen-Huai Song provided the  
595 measurement data.

596

597 *Competing interests.* The authors declare that they have no conflict of interest.

598

599 *Acknowledgements.* We sincerely thank the captain and all crews of the *Dong Fang*

600 *Hong 2*; Wen-shuai Li and Tian-tian Liu from the Ocean University of China for their  
601 help in the research cruise; Yi-xuan Zhang, Yan Fang, Sheng-cheng Shao, Xia Wu and  
602 Tong Huang from Nanjing University of Information Science & Technology for their  
603 assistance in the aerosol sampling and experiment process.

604

605 *Financial support.* This study was financially supported by National Natural Science  
606 Foundation of China (No. 42325304 and 41977185).

607

## 608 **References**

609 Barsanti, K., and Pankow, J.: Thermodynamics of the formation of atmospheric organic particulate  
610 matter by accretion reactions—Part 3: Carboxylic and dicarboxylic acids, *Atmospheric*  
611 *Environment*, 40, 6676-6686, <https://doi.org/10.1016/j.atmosenv.2006.03.013>, 2006.

612 Bates, T., Calhoun, J., and Quinn, P.: Variations in the methanesulfonate to sulfate molar ratio in  
613 marine aerosol particles over the South Pacific Ocean, *Journal of Geophysical Research*, 97,  
614 9859-9865, <https://doi.org/10.1029/92JD00411>, 1992.

615 Bates, T. S., Quinn, P. K., Frossard, A. A., Russell, L. M., Hakala, J., Petäjä, T., Kulmala, M.,  
616 Covert, D. S., Cappa, C. D., Li, S. M., Hayden, K. L., Nuaaman, I., McLaren, R., Massoli, P.,  
617 Canagaratna, M. R., Onasch, T. B., Sueper, D., Worsnop, D. R., and Keene, W. C.: Measurements  
618 of ocean derived aerosol off the coast of California, *Journal of Geophysical Research:*  
619 *Atmospheres*, 117, n/a-n/a, <https://doi.org/10.1029/2012jd017588>, 2012.

620 Bauer, H., Claeys, M., Vermeylen, R., Schüller, E., Weinke, G., Berger, A., and Puxbaum, H.:  
621 Arabitol and mannitol as tracers for a quantification of airborne fungal spores, *Atmospheric*  
622 *Environment*, 42, 588-593, <https://doi.org/10.1016/j.atmosenv.2007.10.013>, 2008.

623 Behera, S. N., Sharma, M., Aneja, V. P., and Balasubramanian, R.: Ammonia in the atmosphere: a  
624 review on emission sources, atmospheric chemistry and deposition on terrestrial bodies, *Environ.*  
625 *Sci. Pollut. Res.*, 20, 8092-8131, <https://doi.org/10.1007/s11356-013-2051-9>, 2013.

626 Bzdek, B., Ridge, D., and Johnston, M.: Amine exchange into ammonium bisulfate and  
627 ammonium nitrate nuclei, *Atmospheric Chemistry and Physics Discussions*, 10, 45-68,  
628 <https://doi.org/10.5194/acpd-10-45-2010>, 2010.

629 Calderón, S., Poor, N., and Campbell, S.: Estimation of the particle and gas scavenging  
630 contributions to wet deposition of organic nitrogen, *Atmospheric Environment*, 41, 4281-4290,  
631 <https://doi.org/10.1016/j.atmosenv.2006.06.067>, 2007.

632 Cao, F., Zhang, Y.-X., Zhang, Y.-L., Song, W.-H., Zhang, Y.-X., Lin, Y.-C., Gul, C., and Haque, M.  
633 M.: Molecular compositions of marine organic aerosols over the Bohai and Yellow Seas: Influence  
634 of primary emission and secondary formation, *Atmospheric Research*, 297, 107088,  
635 <https://doi.org/10.1016/j.atmosres.2023.107088>, 2024.

636 Carpenter, L., Archer, S., and Beale, R.: Ocean-atmosphere trace gas exchange, *Chemical Society*  
637 *reviews*, 41, 6473-6506, <https://doi.org/10.1039/c2cs35121h>, 2012.

638 Chan, L., and Chan, C.: Role of the Aerosol Phase State in Ammonia/Amines Exchange Reactions,  
639 *Environmental science & technology*, 47, 5755-5762, <https://doi.org/10.1021/es4004685>, 2013.

640 Chen, D., Yao, X., Chan, C. K., Tian, X., Chu, Y., Clegg, S. L., Shen, Y., Gao, Y., and Gao, H.:  
641 Competitive Uptake of Dimethylamine and Trimethylamine against Ammonia on Acidic Particles  
642 in Marine Atmospheres, *Environmental Science & Technology*, 56, 5430-5439,  
643 <https://doi.org/10.1021/acs.est.1c08713>, 2022.

644 Chen, Y., Patel, N., Crombie, A., Scrivens, J., and Murrell, J.: Bacterial flavin-containing  
645 monooxygenase is trimethylamine monooxygenase, *Proceedings of the National Academy of*  
646 *Sciences of the United States of America*, 108, 17791-17796,  
647 <https://doi.org/10.1073/pnas.1112928108>, 2011.

648 Chen, Y., Tian, M., Shi, G., Wang, H., Peng, C., Cao, J., Wang, Q., Zhang, S., Guo, D., Zhang, L.,  
649 and Yang, F.: Characterization of urban amine-containing particles in southwestern China:  
650 Seasonal variation, source, and processing, *Atmospheric Chemistry and Physics*, 19, 3245-3255,  
651 <https://doi.org/10.5194/acp-19-3245-2019>, 2019.

652 Cheng, C., Huang, Z., Chan, C., Chu, Y., Li, M., Zhang, T., Ou, Y., Chen, D., Cheng, P., Lei, L.,  
653 Gao, W., Huang, Z., Huang, B., Fu, Z., and Zhou, Z.: Characteristics and mixing state of  
654 amine-containing particles at a rural site in the Pearl River Delta, China, *Atmospheric Chemistry*  
655 *and Physics*, 18, 9147-9159, <https://doi.org/10.5194/acp-18-9147-2018>, 2018.

656 Cheng, G., Hu, Y., Sun, M., Chen, Y., Chen, Y., Zong, C., Chen, J., and Ge, X.: Characteristics and  
657 potential source areas of aliphatic amines in PM<sub>2.5</sub> in Yangzhou, China, *Atmospheric Pollution*  
658 *Research*, 11, 296-302, <https://doi.org/10.1016/j.apr.2019.11.002>, 2020.

659 Chu, Y., Sauerwein, M., and Chan, C. K.: Hygroscopic and phase transition properties of alkyl  
660 aminium sulfates at low relative humidities, *Physical Chemistry Chemical Physics*, 17,  
661 19789-19796, <https://doi.org/10.1039/C5CP02404H>, 2015.

662 Corral, A. F., Choi, Y., Collister, B. L., Crosbie, E., Dadashazar, H., DiGangi, J. P., Diskin, G. S.,  
663 Fenn, M., Kirschler, S., Moore, R. H., Nowak, J. B., Shook, M. A., Stahl, C. T., Shingler, T.,  
664 Thornhill, K. L., Voigt, C., Ziemba, L. D., and Sorooshian, A.: Dimethylamine in cloud water: a  
665 case study over the northwest Atlantic Ocean, *Environmental Science: Atmospheres*, 2, 1534-1550,  
666 <https://doi.org/10.1039/D2EA00117A>, 2022.

667 Dall'osto, M., Airs, R., Beale, R., Cree, C., Fitzsimons, M., Beddows, D., Harrison, R., Ceburnis,  
668 D., O'Dowd, C., Rinaldi, M., Paglione, M., Nenes, A., Decesari, S., and Simó, R.: Simultaneous  
669 Detection of Alkylamines in the Surface Ocean and Atmosphere of the Antarctic Sympagic

670 Environment, ACS Earth and Space Chemistry, 3, 854-862,  
671 <https://doi.org/10.1021/acsearthspacechem.9b00028>, 2019.

672 Du, W., Wang, X., Yang, F., Bai, K., Wu, C., Liu, S., Wang, F., Lv, S., Chen, Y., Wang, J., Liu, W.,  
673 Wang, L., Chen, X., and Wang, G.: Particulate Amines in the Background Atmosphere of the  
674 Yangtze River Delta, China: Concentration, Size Distribution, and Sources, Advances in  
675 Atmospheric Sciences, 38, 1128-1140, <https://doi.org/10.1007/s00376-021-0274-0>, 2021.

676 Facchini, M., Decesari, S., Rinaldi, M., Carbone, C., Finessi, E., Mircea, M., Sandro, F., Moretti,  
677 F., Tagliavini, E., Ceburnis, D., and O'Dowd, C.: Important Source of Marine Secondary Organic  
678 Aerosol from Biogenic Amines, Environmental science & technology, 42, 9116-9121,  
679 <https://doi.org/10.1021/es8018385>, 2008a.

680 Facchini, M., Rinaldi, M., Decesari, S., Carbone, C., Finessi, E., Mircea, M., Sandro, F., Ceburnis,  
681 D., Flanagan, R., Nilsson, E., de Leeuw, G., Martino, M., Woeltjen, J., and Dowd, C.: Primary  
682 submicron marine aerosol dominated by insoluble organic colloids and aggregates, Geophysical  
683 Research Letters, 35, L17814, <https://doi.org/10.1029/2008GL034210>, 2008b.

684 Fan, M.-Y., Zhang, Y.-L., Lin, Y.-C., Chang, Y.-H., Cao, F., Zhang, W.-Q., Hu, Y.-B., Bao, M.-Y.,  
685 Liu, X.-Y., Zhai, X.-Y., Lin, X., Zhao, Z.-Y., and Song, W.-H.: Isotope-based source  
686 apportionment of nitrogen-containing aerosols: A case study in an industrial city in China,  
687 Atmospheric Environment, 212, 96-105, <https://doi.org/10.1016/j.atmosenv.2019.05.020>, 2019.

688 Fang, Y., Chen, Y., Tian, C., Lin, T., Hu, L., Li, J., and Zhang, G.: Application of PMF receptor  
689 model merging with PAHs signatures for source apportionment of black carbon in the continental  
690 shelf surface sediments of the Bohai and Yellow Seas, China, Journal of Geophysical Research:  
691 Oceans, 121, 1346-1359, <https://doi.org/10.1002/2015JC011214>, 2016.

692 Feng, H., Ye, X., Liu, Y., Wang, Z., Gao, T., Cheng, A., and Chen, J.: Simultaneous Determination  
693 of Nine Atmospheric Amines and Six Inorganic Ions by Non-suppressed Ion Chromatography  
694 Using Acetonitrile and 18-Crown-6 as Eluent Additive, Journal of Chromatography A, 461234,  
695 <https://doi.org/10.1016/j.chroma.2020.461234>, 2020.

696 Feng, X., Wang, C., Feng, Y., Junjie, C., Zhang, Y., Qi, X., Li, Q., Li, J., and Chen, Y.: Outbreaks  
697 of Ethyl-Amines during Haze Episodes in North China Plain: A Potential Source of Amines from  
698 Ethanol Gasoline Vehicle Emission, Environmental Science & Technology Letters, 9, 306-311,  
699 <https://doi.org/10.1021/acs.estlett.2c00145>, 2022.

700 Gaston, C., Quinn, P., Bates, T., Gilman, J., Bon, D., Kuster, W., and Prather, K.: The impact of  
701 shipping, agricultural, and urban emissions on single particle chemistry observed aboard the R/V  
702 Atlantis during CalNex, Journal of Geophysical Research: Atmospheres, 118, 5003-5017,  
703 <https://doi.org/10.1002/jgrd.50427>, 2013.

704 Ge, X., Wexler, A., and Clegg, S.: Atmospheric amines – Part I. A review, Atmospheric  
705 Environment, 45, 524-546, <https://doi.org/10.1016/j.atmosenv.2010.10.012>, 2011a.

706 Ge, X., Wexler, A., and Clegg, S.: Atmospheric amines – Part II. Thermodynamic properties and  
707 gas/particle partitioning, Atmospheric Environment, 45, 561-577,

708 <https://doi.org/10.1016/j.atmosenv.2010.10.013>, 2011b.

709 Gibb, S., Mantoura, R., and Liss, P.: Ocean-atmosphere exchange and atmospheric speciation of  
710 ammonia and methylamines in the region of the NW Arabian Sea, *Global Biogeochemical Cycles*  
711 - GLOBAL BIOGEOCHEM CYCLE, 13, 161-178, <https://doi.org/10.1029/98GB00743>, 1999.

712 Gomez-Hernandez, M., McKeown, M., Secrest, J., Marrero-Ortiz, W., Lavi, A., Rudich, Y.,  
713 Collins, D. R., and Zhang, R.: Hygroscopic Characteristics of Alkylammonium Carboxylate Aerosols,  
714 *Environmental Science & Technology*, 50, 2292-2300, <https://doi.org/10.1021/acs.est.5b04691>,  
715 2016.

716 Gorzelska, K., and Galloway, J.: Amine nitrogen in the atmospheric environment over the North  
717 Atlantic Ocean, *Global Biogeochemical Cycles - GLOBAL BIOGEOCHEM CYCLE*, 4, 309-333,  
718 <https://doi.org/10.1029/GB004i003p00309>, 1990.

719 Haque, M., Kawamura, K., Deshmukh, D., Cao, F., Song, W., Bao, M., and Zhang, Y.:  
720 Characterization of organic aerosols from a Chinese megacity during winter: Predominance of  
721 fossil fuel combustion, *Atmospheric Chemistry and Physics*, 19, 5147-5164,  
722 <https://doi.org/10.5194/acp-19-5147-2019>, 2019.

723 He, Q., Ding, X., Fu, X.-X., Zhang, Y.-Q., Wang, J.-Q., Liu, Y.-X., Tang, M.-J., Wang, X., and  
724 Rudich, Y.: Secondary Organic Aerosol Formation from Isoprene Epoxides in the Pearl River  
725 Delta, South China: IEPOX- and HMML-Derived Tracers, *Journal of Geophysical Research:*  
726 *Atmospheres*, 123, 6999-7012, <https://doi.org/10.1029/2017JD028242>, 2018.

727 Hemmilä, M., Hellén, H., Virkkula, A., Makkonen, U., Praplan, A., Kontkanen, J., Ahonen, L.,  
728 Kulmala, M., and Hakola, H.: Amines in boreal forest air at SMEAR II station in Finland,  
729 *Atmospheric Chemistry and Physics*, 18, 6367-6380, <https://doi.org/10.5194/acp-18-6367-2018>,  
730 2018.

731 Hu, Q., Yu, P., Zhu, Y., Li, K., Gao, H., and Yao, X.: Concentration, Size Distribution, and  
732 Formation of Trimethylammonium and Dimethylammonium Ions in Atmospheric Particles over  
733 Marginal Seas of China\*, *Journal of the Atmospheric Sciences*, 72, 150522112638006,  
734 <https://doi.org/10.1175/JAS-D-14-0393.1>, 2015.

735 Huang, S., Song, Q., Hu, W., Yuan, B., Liu, J., Jiang, B., Li, W., Wu, C., Jiang, F., Chen, W., Wang,  
736 X., and Shao, M.: Chemical composition and sources of amines in PM<sub>2.5</sub> in an urban site of PRD,  
737 China, *Environmental Research*, 212, 113261, <https://doi.org/10.1016/j.envres.2022.113261>, 2022.

738 Huang, X., Kao, S.-J., Lin, J., Qin, X., and Deng, C.: Development and validation of a HPLC/FLD  
739 method combined with online derivatization for the simple and simultaneous determination of  
740 trace amino acids and alkyl amines in continental and marine aerosols, *PLOS ONE*, 13, e0206488,  
741 <https://doi.org/10.1371/journal.pone.0206488>, 2018.

742 Johnson, J., and Jen, C.: Role of Methanesulfonic Acid in Sulfuric Acid–Amine and Ammonia  
743 New Particle Formation, *ACS Earth and Space Chemistry*, 7, 653-660,  
744 <https://doi.org/10.1021/acsearthspacechem.3c00017>, 2023.

745 Kanawade, V. P., and Jokinen, T.: Atmospheric amines are a crucial yet missing link in Earth's

746 climate via airborne aerosol production, *Commun Earth Environ*, 6, 98,  
747 <https://doi.org/10.1038/s43247-025-02063-0>, 2025.

748 Kang, M., Fu, P., Kawamura, K., Yang, F., Zhang, H., Zang, Z., Ren, H., Ren, L., Zhao, y., Sun, Y.,  
749 and Wang, Z.: Characterization of biogenic primary and secondary organic aerosols in the marine  
750 atmosphere over the East China Sea, *Atmospheric Chemistry and Physics*, 18, 13947-13967,  
751 <https://doi.org/10.5194/acp-18-13947-2018>, 2018.

752 Kleindienst, T., Jaoui, M., Lewandowski, M., Offenber, J., Lewis, C., Bhave, P., and Edney, E.:  
753 Estimates of the contributions of biogenic and anthropogenic hydrocarbons to secondary organic  
754 aerosol at a southern US location, *Atmospheric Environment*, 41, 8288-8300,  
755 <https://doi.org/10.1016/j.atmosenv.2007.06.045>, 2007.

756 Köllner, F., Schneider, J., Willis, M., Klimach, T., Helleis, F., Bozem, H., Kunkel, D., Hoor, P.,  
757 Burkart, J., Leaitch, W. R., Aliabadi, A. A., Abbatt, J., Herber, Andreas B., and Borrmann, S.:  
758 Particulate trimethylamine in the summertime Canadian high Arctic lower troposphere,  
759 *Atmospheric Chemistry and Physics*, 17, 13747-13766,  
760 <https://doi.org/10.5194/acp-17-13747-2017>, 2017.

761 Lee, D., and Wexler, A.: Atmospheric amines – Part III: Photochemistry and toxicity, *Atmospheric*  
762 *Environment*, 71, 95–103, <https://doi.org/10.1016/j.atmosenv.2013.01.058>, 2013.

763 Li, G., Liao, Y., Hu, J., Lu, L., Zhang, Y., Li, B., and An, T.: Activation of NF- $\kappa$ B pathways  
764 mediating the inflammation and pulmonary diseases associated with atmospheric methylamine  
765 exposure, *Environmental Pollution*, 252, 1216-1224, <https://doi.org/10.1016/j.envpol.2019.06.059>,  
766 2019a.

767 Li, J., Wang, G., Zhang, q., Li, J., wu, C., Jiang, W., Zhu, T., and Zeng, L.: Molecular  
768 characteristics and diurnal variations of organic aerosols at a rural site in the North China Plain  
769 with implications for the influence of regional biomass burning, *Atmospheric Chemistry and*  
770 *Physics*, 19, 10481-10496, <https://doi.org/10.5194/acp-19-10481-2019>, 2019b.

771 Lidbury, I., Chen, Y., and Murrell, J.: Trimethylamine and trimethylamine N-oxide are  
772 supplementary energy sources for a marine heterotrophic bacterium: Implications for marine  
773 carbon and nitrogen cycling, *The ISME Journal*, 9, 760-769,  
774 <https://doi.org/10.1038/ismej.2014.149>, 2015.

775 Lidbury, I., Matusz, M., Scanlan, D., and Chen, Y.: Identification of dimethylamine  
776 monooxygenase in marine bacteria reveals a metabolic bottleneck in the methylated amine  
777 degradation pathway, *The ISME Journal*, 11, 1592-1601, <https://doi.org/10.1038/ismej.2017.31>,  
778 2017.

779 Lin, P., Laskin, J., Nizkorodov, S., and Laskin, A.: Revealing Brown Carbon Chromophores  
780 Produced in Reactions of Methylglyoxal with Ammonium Sulfate, *Environmental science &*  
781 *technology*, 49, 14257-14266, <https://doi.org/10.1021/acs.est.5b03608>, 2015.

782 Lin, Q., Zhang, G., Long, P., Bi, X., Wang, X., Brechtel, F., Li, M., Chen, D., Peng, P., amp, apos,  
783 an, Sheng, G., and Zhou, Z.: In situ chemical composition measurement of individual cloud

784 residue particles at a mountain site, southern China, *Atmospheric Chemistry and Physics*, 17,  
785 8473-8488, 2017.

786 Liu, F., Bi, X., Zhang, G., Peng, L., Lian, X., Lu, H., Fu, Y., Wang, X., Peng, P. a., and Sheng, G.:  
787 Concentration, size distribution and dry deposition of amines in atmospheric particles of urban  
788 Guangzhou, China, *Atmospheric Environment*, 171, 279-288,  
789 <https://doi.org/10.1016/j.atmosenv.2017.10.016>, 2017.

790 Liu, F., Bi, X., Zhang, G., Lian, X., Fu, Y., Yang, Y., Lin, Q., Jiang, F., Wang, X., Peng, P. a., and  
791 Sheng, G.: Gas-to-particle partitioning of atmospheric amines observed at a mountain site in  
792 southern China, *Atmospheric Environment*, 195, 1-11,  
793 <https://doi.org/10.1016/j.atmosenv.2018.09.038>, 2018.

794 Liu, T., Xu, Y., Sun, Q., Zhu, R.-G., Li, C. X., Li, Z. Y., Zhang, K. Q., Sun, C. X., and Xiao, H. Y.:  
795 Characteristics, Origins, and Atmospheric Processes of Amines in Fine Aerosol Particles in Winter  
796 in China, *Journal of Geophysical Research: Atmospheres*, 128, e2023JD038974,  
797 <https://doi.org/10.1029/2023JD038974>, 2023.

798 Liu, Z., Li, M., Wang, X., Liang, Y., Jiang, Y., Chen, J., Mu, J., Zhu, Y., Meng, H., Yang, L., Hou,  
799 K., Wang, Y., and Xue, L.: Large contributions of anthropogenic sources to amines in fine particles  
800 at a coastal area in northern China in winter, *Science of The Total Environment*, 839, 156281,  
801 <https://doi.org/10.1016/j.scitotenv.2022.156281>, 2022.

802 Marrero-Ortiz, W., Hu, M., Du, Z., Ji, Y.-M., Wang, Y., Guo, S., Lin, Y., Gomez-Hernandez, M.,  
803 Peng, J., Li, Y., Secret, J., Levy Zamora, M., Wang, Y., An, T., and Zhang, R.: Formation and  
804 Optical Properties of Brown Carbon from Small  $\alpha$ -Dicarbonyls and Amines, *Environmental*  
805 *Science & Technology*, 53, 117-126, <https://doi.org/10.1021/acs.est.8b03995>, 2018.

806 Medeiros, P., Conte, M., Weber, J., and Simoneit, B.: Sugars as source indicators of biogenic  
807 organic carbon in aerosols collected above the Howland Experimental Forest, Maine, *Atmospheric*  
808 *Environment*, 40, 1694-1705, <https://doi.org/10.1016/j.atmosenv.2005.11.001>, 2006.

809 Milne, P., and Zika, R.: Amino acid nitrogen in atmospheric aerosols: Occurrence, sources and  
810 photochemical modification, *Journal of Atmospheric Chemistry*, 16, 361-398,  
811 <https://doi.org/10.1007/BF01032631>, 1993.

812 Miyazaki, Y., Kawamura, K., and Sawano, M.: Size distributions and chemical characterization of  
813 water-soluble organic aerosols over the western North Pacific in summer, *Journal of Geophysical*  
814 *Research*, 115, 210, <https://doi.org/10.1029/2010JD014439>, 2010.

815 Mochida, M., Kawabata, A., Kawamura, K., Hatsushika, H., and Yamazaki, K.: Seasonal variation  
816 and origin of dicarboxylic acids in the marine atmosphere over the western North Pacific, *Journal*  
817 *of Geophysical Research*, 108, 4193, <https://doi.org/10.1029/2002JD002355>, 2003.

818 Müller, C., Iinuma, Y., Karstensen, J., Pinxteren, D., S, L., T, G., and Herrmann, H.: Seasonal  
819 variation of aliphatic amines in marine sub-micrometer particles at the Cape Verde Islands,  
820 *Atmospheric Chemistry and Physics*, 9, 9587-9597, <https://doi.org/10.5194/acpd-9-14825-2009>,  
821 2009.

822 Myriokefalitakis, S., Elisabetta, V., Tsigaridis, K., Papadimas, C. D., Sciare, J., Mihalopoulos, N.,  
823 Facchini, M., Matteo, R., Dentener, F., Ceburnis, D., Hatzianastassiou, N., O'Dowd, C., van Weele,  
824 M., and Kanakidou, M.: Global Modeling of the Oceanic Source of Organic Aerosols, *Advances*  
825 *in Meteorology*, 2010, 2010, <https://doi.org/10.1155/2010/939171>, 2010.

826 Nakamura, T., Matsumoto, K., and Uematsu, M.: Chemical characteristics of aerosols transported  
827 from Asia to the East China Sea: An evaluation of anthropogenic combined nitrogen deposition in  
828 autumn, *Atmospheric Environment*, 39, 1749-1758,  
829 <https://doi.org/10.1016/j.atmosenv.2004.11.037>, 2005.

830 Namieśnik, J., Jastrzebska, A., and Zygmunt, B.: Determination of volatile aliphatic amines in air  
831 by solid-phase microextraction coupled with gas chromatography with flame ionization detection,  
832 *Journal of chromatography. A*, 1016, 1-9, [https://doi.org/10.1016/S0021-9673\(03\)01296-2](https://doi.org/10.1016/S0021-9673(03)01296-2), 2003.

833 Ng, N., Jimenez, J., Chhabra, P., Seinfeld, J., and Worsnop, D.: Changes in organic aerosol  
834 composition with aging inferred from aerosol mass spectra, *Atmospheric Chemistry and Physics -*  
835 *ATMOS CHEM PHYS*, 11, 6465-6474, <https://doi.org/10.5194/acp-11-6465-2011>, 2011.

836 Nielsen, C. J., Herrmann, H., and Weller, C.: Atmospheric chemistry and environmental impact of  
837 the use of amines in carbon capture and storage (CCS), *Chem Soc Rev*, 41, 6684-6704,  
838 <https://doi.org/10.1039/c2cs35059a>, 2012.

839 Pankow, J.: Phase Considerations in the Gas/Particle Partitioning of Organic Amines in the  
840 Atmosphere, *Atmospheric Environment*, 122, 448-453,  
841 <https://doi.org/10.1016/j.atmosenv.2015.09.056>, 2015.

842 Pinxteren, M. V., Fomba, K., Pinxteren, D., Triesch, N., Hoffmann, E., Cree, C., Fitzsimons, M.,  
843 Tümpling, W., and Herrmann, H.: Aliphatic amines at the Cape Verde Atmospheric Observatory:  
844 Abundance, origins and sea-air fluxes, *Atmospheric Environment*, 203, 183-195,  
845 <https://doi.org/10.1016/j.atmosenv.2019.02.011>, 2019.

846 Place, B., Quilty, A., Lorenzo, R., Ziegler, S., and VandenBoer, T.: Quantitation of 11 alkyl amines  
847 in atmospheric samples: Separating structural isomers by ion chromatography, *Atmospheric*  
848 *Measurement Techniques*, 10, 1061-1078, <https://doi.org/10.5194/amt-10-1061-2017>, 2017.

849 Price, D., Clark, C., Tang, X., Cocker, D., Purvis-Roberts, K., and Silva, P.: Proposed chemical  
850 mechanisms leading to secondary organic aerosol in the reactions of aliphatic amines with  
851 hydroxyl and nitrate radicals, *Atmospheric Environment*, 96, 135-144,  
852 <https://doi.org/10.1016/j.atmosenv.2014.07.035>, 2014.

853 Price, D., Kacarab, M., Cocker, D., Purvis-Roberts, K., and Silva, P.: Effects of Temperature on  
854 the Formation of Secondary Organic Aerosol from Amine Precursors, *Aerosol Science and*  
855 *Technology*, 50, 1216-1226, <https://doi.org/10.1080/02786826.2016.1236182>, 2016.

856 Qiu, C., and Zhang, R.: Multiphase chemistry of atmospheric amines, *Physical chemistry chemical*  
857 *physics*, 15, 5738-5752, <https://doi.org/10.1039/c3cp43446j>, 2013.

858 Rinaldi, M., Decesari, S., Finessi, E., Giulianelli, L., Carbone, C., Fuzzi, S., O'Dowd, C. D.,  
859 Ceburnis, D., and Facchini, M. C.: Primary and Secondary Organic Marine Aerosol and Oceanic

860 Biological Activity: Recent Results and New Perspectives for Future Studies, *Advances in*  
861 *Meteorology*, 2010, 1-10, <https://doi.org/10.1155/2010/310682>, 2010.

862 Rogge, W., Hildemann, L., Mazurek, M., Cass, G., and Simoneit, B.: Sources of Fine Organic  
863 Aerosol. 3. Road Dust, Tire Debris, and Organometallic Brake Lining Dust: Roads as Sources and  
864 Sinks, *Environmental Science & Technology - ENVIRON SCI TECHNOL*, 27, 1892-1904,  
865 <https://doi.org/10.1021/es00046a019>, 1993.

866 Schade, G., and Crutzen, P.: Emission of aliphatic amines from animal husbandry and their  
867 reactions: Potential source of N<sub>2</sub>O and HCN, *Journal of Atmospheric Chemistry*, 22, 319-346,  
868 <https://doi.org/10.1007/BF00696641>, 1995.

869 Shen, J., Xie, H.-B., Elm, J., ma, F., Chen, J., and Vehkamäki, H.: Methanesulfonic Acid-driven  
870 New Particle Formation Enhanced by Monoethanolamine: A Computational Study, *Environmental*  
871 *Science & Technology*, 53, 14387-14397, <https://doi.org/10.1021/acs.est.9b05306>, 2019.

872 Shen, W., Ren, L., Zhao, Y., Zhou, L., Dai, L., Ge, X., Kong, S., Yan, Q., Xu, H., Jiang, Y., He, J.,  
873 Chen, M., and Yu, H.: C1-C2 alkyl aminiums in urban aerosols: Insights from ambient and fuel  
874 combustion emission measurements in the Yangtze River Delta region of China, *Environ Pollut*,  
875 230, 12-21, <https://doi.org/10.1016/j.envpol.2017.06.034>, 2017.

876 Shen, X., Chen, J., and An, T.: A new advance in pollution profile, transformation process, and  
877 contribution to SOA formation of atmospheric organic amines, *Environmental Science:*  
878 *Atmospheres*, 3, 444-473, <https://doi.org/10.1039/D2EA00167E>, 2023.

879 Simoneit, B., Sheng, G., Chen, X., Fu, J., Zhang, J., and Xu, Y.: Molecular marker study of  
880 extractable organic matter in aerosols from urban areas of China, *Atmospheric Environment. Part*  
881 *A. General Topics*, 25, 2111-2129, [https://doi.org/10.1016/0960-1686\(91\)90088-O](https://doi.org/10.1016/0960-1686(91)90088-O), 1991.

882 Simoneit, B., Elias, V., Kobayashi, M., Kawamura, K., Rushdi, A., Medeiros, P., Rogge, W., and  
883 Didyk, B.: Sugars Dominant Water-Soluble Organic Compounds in Soils and Characterization as  
884 Tracers in Atmospheric Particulate Matter, *Environmental science & technology*, 38, 5939-5949,  
885 <https://doi.org/10.1021/es0403099>, 2004.

886 Sorooshian, A., Murphy, S., Hersey, S., H, G., Padro, L., Nenes, A., Brechtel, F., Jonsson, H.,  
887 Flagan, R., and Seinfeld, J.: Comprehensive airborne characterization of aerosol from a major  
888 bovine source, *Atmospheric Chemistry and Physics Discussions*, 8, 10415-10479,  
889 <https://doi.org/10.5194/acp-8-5489-2008>, 2008.

890 Sun, J., Matusz, M., Chen, Y., and Giovannoni, S.: Microbial Trimethylamine Metabolism in  
891 Marine Environments: Microbial TMA metabolism, *Environmental Microbiology*, 21, 513-520,  
892 <https://doi.org/10.1111/1462-2920.14461>, 2019.

893 Tang, X., Price, D., Praske, E., Lee, S. A., Shattuck, M. A., Purvis-Roberts, K., Silva, P. J.,  
894 Asa-Awuku, A., and Cocker, D. R.: NO<sub>3</sub> radical, OH radical and O<sub>3</sub>-initiated secondary aerosol  
895 formation from aliphatic amines, *Atmospheric Environment*, 72, 105-112,  
896 <https://doi.org/10.1016/j.atmosenv.2013.02.024>, 2013.

897 Tang, X., Price, D., Praske, E., Vu, D. N., Purvis-Roberts, K., Silva, P. J., Cocker Iii, D. R., and

898 Asa-Awuku, A.: Cloud condensation nuclei (CCN) activity of aliphatic amine secondary aerosol,  
899 Atmospheric Chemistry and Physics, 14, 5959-5967, <https://doi.org/10.5194/acp-14-5959-2014>,  
900 2014.

901 Van Neste, A., Duce, R. A., and Lee, C.: Methylamines in the Marine Atmosphere, Geophysical  
902 Research Letters - GEOPHYS RES LETT, 14, 711-714,  
903 <https://doi.org/10.1029/GL014i007p00711>, 1987.

904 VandenBoer, T., Markovic, M., Petroff, A., Czar, M. F., Borduas, N., and Murphy, J. G.: Ion  
905 chromatographic separation and quantitation of alkyl methylamines and ethylamines in  
906 atmospheric gas and particulate matter using preconcentration and suppressed conductivity  
907 detection, Journal of chromatography. A, 1252, 74-83,  
908 <https://doi.org/10.1016/j.chroma.2012.06.062>, 2012.

909 Violaki, K., and Mihalopoulos, N.: Water-soluble organic nitrogen (WSON) in size-segregated  
910 atmospheric particles over the Eastern Mediterranean, Atmospheric Environment, 44, 4339-4345,  
911 <https://doi.org/10.1016/j.atmosenv.2010.07.056>, 2010.

912 Wang, X.-C., and Lee, C.: Sources and distribution of aliphatic amines in salt marsh sediment,  
913 Organic Geochemistry - ORG GEOCHEM, 22, 1005-1021,  
914 [https://doi.org/10.1016/0146-6380\(94\)90034-5](https://doi.org/10.1016/0146-6380(94)90034-5), 1994.

915 Welsh, D.: Ecological significance of compatible solute accumulation by micro-organisms: From  
916 single cells to global climate, FEMS Microbiology Reviews, 24, 263-290,  
917 <https://doi.org/10.1111/j.1574-6976.2000.tb00542.x>, 2000.

918 Xie, H., Feng, L., Hu, Q., Zhu, Y., Gao, H., Gao, Y., and Yao, X.: Concentration and size  
919 distribution of water-extracted dimethylammonium and trimethylammonium in atmospheric particles  
920 during nine campaigns - Implications for sources, phase states and formation pathways, The  
921 Science of the total environment, 631-632, 130-141,  
922 <https://doi.org/10.1016/j.scitotenv.2018.02.303>, 2018.

923 Yang, H., Xu, J., Wu, W.-S., Wan, C., and Yu, J.: Chemical Characterization of Water-Soluble  
924 Organic Aerosols at Jeju Island Collected During ACE-Asia, Environmental Chemistry -  
925 ENVIRON CHEM, 1, 13-17, <https://doi.org/10.1071/EN04006>, 2004.

926 Yang, X.-Y., Cao, F., Fan, M., Lin, Y. C., Xie, F., and Zhang, Y.: Seasonal variations of low  
927 molecular alkyl amines in PM<sub>2.5</sub> in a North China Plain industrial city: Importance of secondary  
928 formation and combustion emissions, The Science of the total environment, 857, 159371,  
929 <https://doi.org/10.1016/j.scitotenv.2022.159371>, 2023.

930 Yao, L., Garmash, O., Bianchi, F., Zheng, J., Yan, C., Kontkanen, J., Junninen, H., Mazon, S., Ehn,  
931 M., Paasonen, P., Sipilä, M., Wang, M., Wang, X., Xiao, S., Chen, H., Lu, Y., Zhang, B., Wang, D.,  
932 Fu, Q., and Wang, L.: Atmospheric new particle formation from sulfuric acid and amines in a  
933 Chinese megacity, Science, 361, 278-281, <https://doi.org/10.1126/science.aao4839>, 2018.

934 Yin, S., Ge, M.-F., Wang, W., Liu, Z., and Wang, D.: Uptake of gas-phase alkylamines by sulfuric  
935 acid, Chinese Science Bulletin, 56, 1241-1245, <https://doi.org/10.1007/s11434-010-4331-9>, 2011.

936 You, Kanawade, V., de Gouw, J., Guenther, A., Madronich, S., Sierra-Hernández, M., Lawler, M.,  
937 Smith, J., Takahama, S., Ruggeri, G., Koss, A., Olson, K., Baumann, K., Weber, R., Nenes, A.,  
938 Guo, H., Edgerton, E., Porcelli, L., Brune, W., and Lee, S.-H.: Atmospheric amines and ammonia  
939 measured with a Chemical Ionization Mass Spectrometer (CIMS), *Atmospheric Chemistry and*  
940 *Physics*, 14, 12181-12194, <https://doi.org/10.5194/acp-14-12181-2014>, 2014.

941 Yu, P., Hu, Q., Li, K., Zhu, Y., Liu, X., Gao, H., and Yao, X.: Characteristics of dimethylammonium  
942 and trimethylammonium in atmospheric particles ranging from supermicron to nanometer sizes over  
943 eutrophic marginal seas of China and oligotrophic open oceans, *Science of The Total Environment*,  
944 572, 813-824, <https://doi.org/10.1016/j.scitotenv.2016.07.114>, 2016.

945 Zhang, H., Surratt, J., Lin, Y.-H., Bapat, J., and Kamens, R.: Effect of relative humidity on SOA  
946 formation from isoprene/NO photooxidation: Enhancement of 2-methylglyceric acid and its  
947 corresponding oligoesters under dry conditions, *Atmospheric Chemistry and Physics - ATMOS*  
948 *CHEM PHYS*, 11, 6411-6424, <https://doi.org/10.5194/acp-11-6411-2011>, 2011.

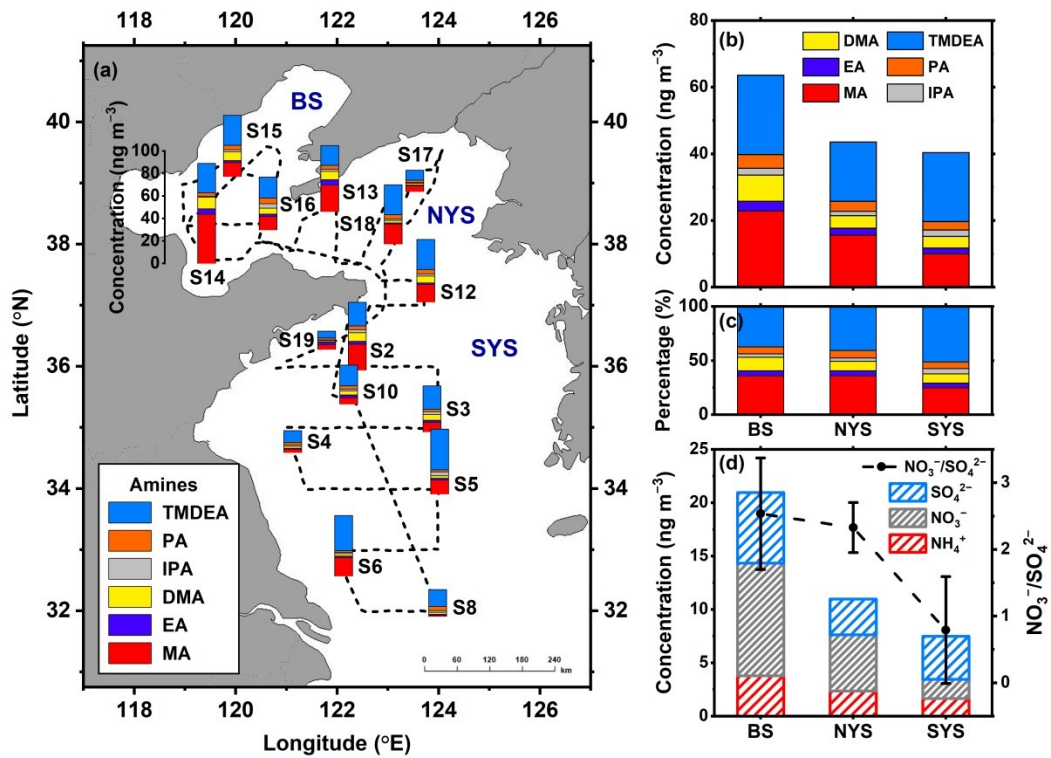
949 Zheng, J., Ma, Y., Chen, M., Zhang, Q., Wang, L., Khalizov, A. F., Yao, L., Wang, Z., Wang, X.,  
950 and Chen, L.: Measurement of atmospheric amines and ammonia using the high resolution  
951 time-of-flight chemical ionization mass spectrometry, *Atmospheric Environment*, 102, 249-259,  
952 <https://doi.org/10.1016/j.atmosenv.2014.12.002>, 2015.

953 Zheng, L., Yang, X., Lai, S., Ren, H., Yue, S., Zhang, Y., Huang, X., Gao, Y., Sun, Y., Wang, Z.,  
954 and Fu, P.: Impacts of springtime biomass burning in the northern Southeast Asia on marine  
955 organic aerosols over the Gulf of Tonkin, China, *Environmental pollution (Barking, Essex : 1987)*,  
956 237, 285-297, <https://doi.org/10.1016/j.envpol.2018.01.089>, 2018.

957 Zhou, S., Li, H., Yang, T., Chen, Y., Deng, C., Gao, Y., Chen, C., and Xu, J.: Characteristics and  
958 sources of aerosol ammoniums over the eastern coast of China: insights from the integrated  
959 observations in a coastal city, adjacent island and surrounding marginal seas, *Atmospheric*  
960 *Chemistry and Physics*, 19, 10447-10467, <https://doi.org/10.5194/acp-19-10447-2019>, 2019.

961 Zhu, S., Yan, C., Zheng, J., Chen, C., Ning, H., Yang, D., Wang, M., Ma, Y., Zhan, J., Hua, C., Yin,  
962 R., Li, Y., Liu, Y., Jiang, J., Yao, L., Wang, L., Kulmala, M., and Worsnop, D.: Observation and  
963 Source Apportionment of Atmospheric Alkaline Gases in Urban Beijing, *Environmental Science*  
964 *& Technology*, 56, 17545-17555, <https://doi.org/10.1021/acs.est.2c03584>, 2022.

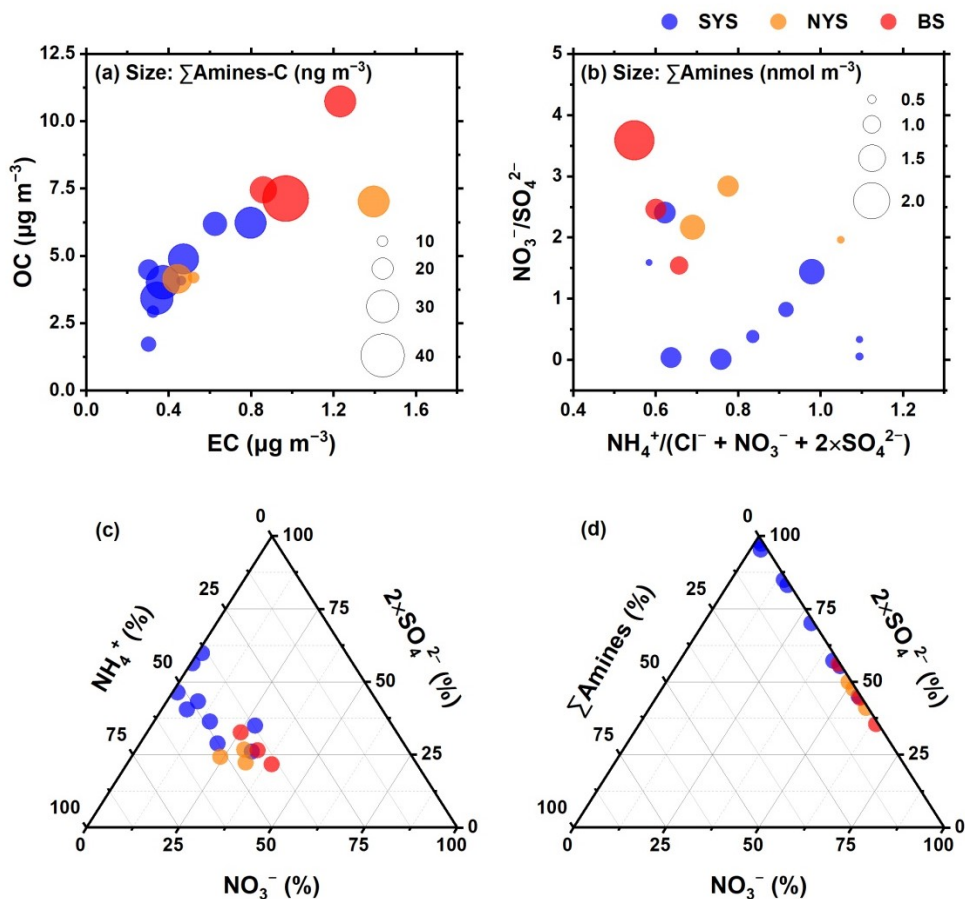
965



966

967 **Figure 1.** Concentrations of amines in 15 TSP samples (a) collected along the cruise  
 968 track (black dotted line); average concentrations (b) and relative contributions (c) of  
 969 amines; and concentrations of NH<sub>4</sub><sup>+</sup>, NO<sub>3</sub><sup>-</sup>, and SO<sub>4</sub><sup>2-</sup>, along with NO<sub>3</sub><sup>-</sup>/SO<sub>4</sub><sup>2-</sup> molar  
 970 ratios (d), in TSP over the SYS, NYS, and BS.

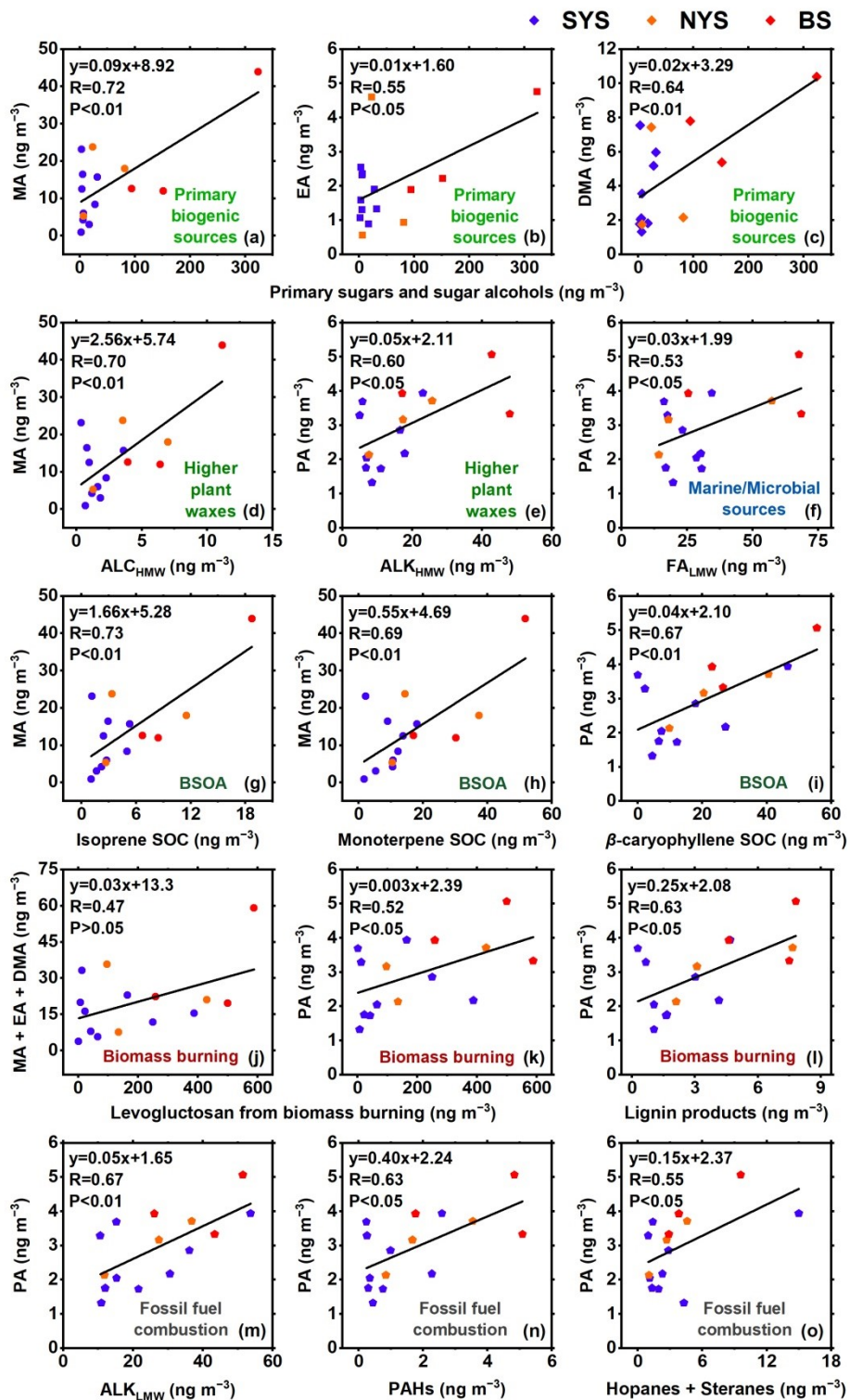
971



972

973 **Figure 2.** Variations of  $\Sigma\text{amines-C}$  with OC and EC concentrations (a); variations of  
 974  $\Sigma\text{amines}$  molar concentrations with the  $\text{NO}_3^-/\text{SO}_4^{2-}$  and  $\text{NH}_4^+ / (\text{Cl}^- + \text{NO}_3^- + 2 \times \text{SO}_4^{2-})$   
 975 molar ratios (b); ternary diagram of the molar ratio of  $\text{NH}_4^+$ ,  $\text{NO}_3^-$ , and  $\text{SO}_4^{2-}$  (c); and  
 976 ternary diagram of the molar ratio of  $\Sigma\text{amines}$ ,  $\text{NO}_3^-$ , and  $\text{SO}_4^{2-}$  (d) in TSP over the  
 977 SYS, NYS, and BS.

978



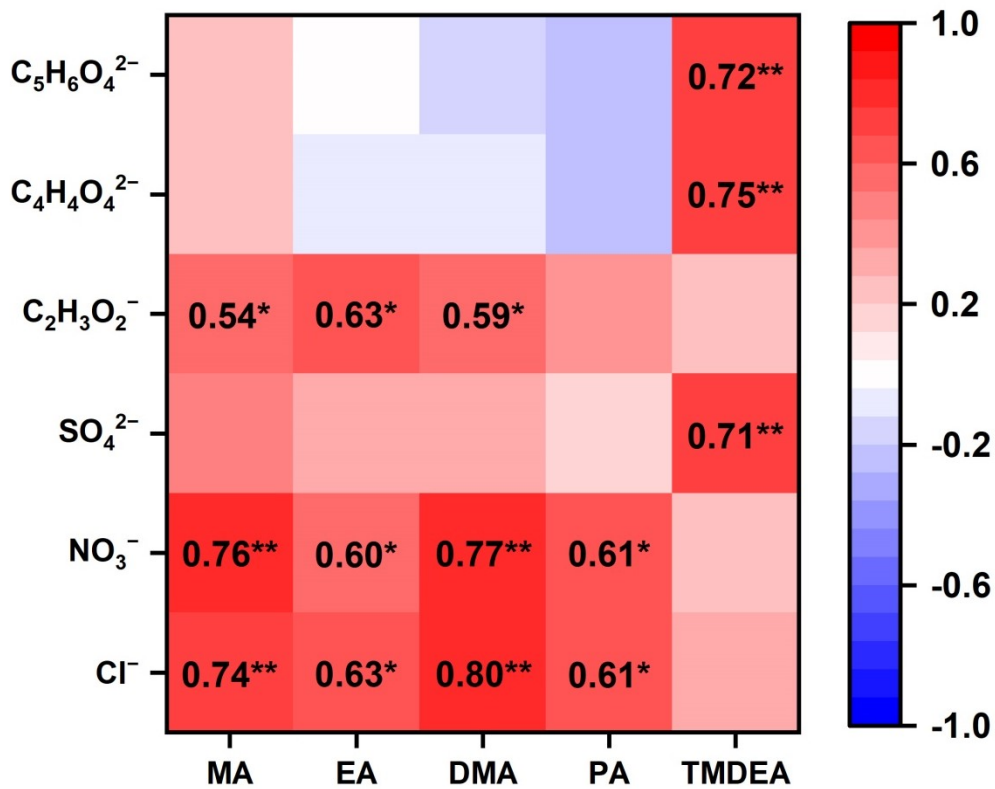
979

980 **Figure 3.** Linear regressions between amines and biomarkers (a–i), biomass burning

981 tracers (j–l), and fossil fuel combustion tracers (m–o) in TSP over the SYS, NYS, and

982 BS.

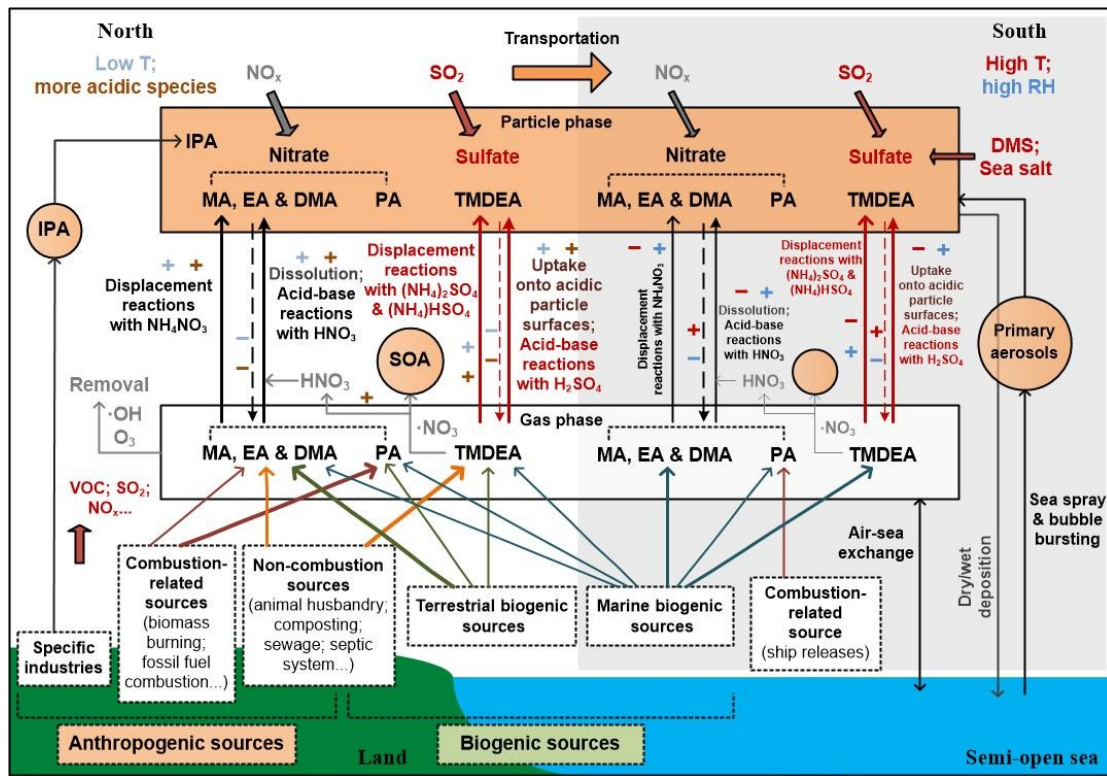
983



984

985 **Figure 4.** Correlation coefficient matrix between amines and acidic species in TSP  
 986 over the YS–BS. Numbers indicate correlation coefficients that passed the  
 987 significance test; \*\* denotes  $P < 0.01$ , and \* denotes  $P < 0.05$ .

988



989

990 **Figure 5.** Schematic diagram illustrating the source contributions and major  
 991 secondary formation mechanisms of amines, along with the influences of  
 992 environmental conditions over the YS-BS.

993